Canadian Science Publishing | **Canadian Journal of Physiology and Pharmacology**

Muscarinic agonists inhibit the ATP-dependent potassium current and suppress the ventricle-Purkinje action potential dispersion

SCHOLARONE™ Manuscripts

1   **Muscarinic agonists inhibit the ATP-dependent potassium current and suppress the**

2   **ventricle-Purkinje action potential dispersion**

3

4   Tibor Magyar[a,§], Tamás Árpádffy-Lovas[a,§], Bence Pászti[a], Noémi Tóth[a], Jozefina Szlovák[a],

5   Péter Gazdag[a], Zsófia Kohajda[b], András Gyökeres[a], Balázs Györe[d], Zsolt Gurabi[a], Norbert

6   Jost[a,b,c], László Virág[a,c], Julius Gy. Papp[a,b], Norbert Nagy[a,b,#], István Koncz[a,*,#]

7

8

9   [a]Department of Pharmacology and Pharmacotherapy, Faculty of Medicine, University of

10   Szeged, Szeged, Hungary;

11   [b]MTA-SZTE Research Group of Cardiovascular Pharmacology, Hungarian Academy of

12   Sciences, Szeged, Hungary

13   [c]Department of Pharmacology and Pharmacotherapy, Interdisciplinary Excellence Centre,

14   University of Szeged, Szeged, Hungary

15   [d]Faculty of Dentistry, University of Szeged, Hungary

16

17   [§] Shared first authorship

18   [#] Shared senior authorship

19

20   *Author for correspondence at:

21   István Koncz MD, PhD

22   Department of Pharmacology & Pharmacotherapy

23   Faculty of Medicine

24   University of Szeged

25   Dóm tér 12,

26   H-6720 Szeged, Hungary

27   E-mail: koncz.istvan@med.u-szeged.hu

28   **Abstract**

29   **Introduction:** Activation of the parasympathetic nervous system has been reported to have an

30   antiarrhythmic role during ischemia-reperfusion injury by decreasing the arrhythmia triggers.

31   Furthermore, it was reported that the parasympathetic neurotransmitter acetylcholine is able to

32   modulate the ATP-dependent K-current ($I_{K\text{-}ATP}$), a crucial current activated during hypoxia.

33   However, the possible significance of this current modulation in the antiarrhythmic

34   mechanism is not fully clarified.

35   **Methods:** Action potentials were measured using the conventional microelectrode technique

36   from canine left ventricular papillary muscle and free-running Purkinje fibers, under normal

37   and hypoxic conditions. Ionic currents were measured using the whole-cell configuration of

38   the patch clamp method.

39   **Results:** 5 μM acetylcholine did not influence the action potential duration (APD) either in

40   Purkinje fibers or in papillary muscle preparations. In contrast, it significantly lengthened the

41   APD and suppressed the Purkinje–ventricle APD dispersion when it was administered after

42   5 μM pinacidil application. 3 μM carbachol reduced the pinacidil-activated $I_{K\text{-}ATP}$ under

43   voltage-clamp condition. Acetylcholine lengthened the ventricular action potential under

44   simulated ischemia condition.

45   **Conclusion:** In this study we found that acetylcholine inhibits the $I_{K\text{-}ATP}$ and thus suppresses

46   the ventricle-Purkinje APD dispersion. We conclude that parasympathetic tone may reduce

47   the arrhythmogenic substrate exerting a complex antiarrhythmic mechanism during hypoxic

48   conditions.

49

50   *Key words:* acetylcholine, Purkinje fibers, papillary muscles, hypoxia

51 **Introduction**

52 The parasympathetic nervous system has a crucial role in controlling the actual heart rate and

53 impulse propagation via influencing the sinoatrial and atrioventricular nodes (Higgins et al.,

54 1973). The parasympathetic nerve endings operate by releasing acetylcholine that acts on

55 M_2-receptors, activating several intracellular signaling routes, and ultimately influencing the

56 cardiac ion channels (Harvey and Belevych, 2003). Even though the parasympathetic nervous

57 system primarily innervates the supraventricular areas of the heart, there are certain important

58 ion channels in the ventricular muscle that are known to be influenced by the release of

59 acetylcholine. It has been previously reported that the inward rectifier potassium current (I_{K1};

60 Koumi et al., 1995) and the slow component of the delayed rectifier (I_{Ks}; Pappano and

61 Carmeliet, 1979) are inhibited, whereas I_{K-ATP} and I_{K-ACh} are activated by acetylcholine via

62 G proteins (Terzic et al, 1994; Ito et al., 1994; Kim et al., 1997).

63

64 The importance of these effects of acetylcholine is underpinned by the fact that the activation

65 of I_{K-ATP} channels is well known during hypoxia/ischemia, in which situations the duration of

66 the action potential is shortened (Weiss and Venkatesh, 1993). Furthermore, it was reported

67 that vagal activation is also facilitated under ischemia–reperfusion (Recordati et al., 1971).

68 This vagal activation during hypoxia could be antiarrhythmic, since it was reported that

69 increased parasympathetic tone reduces the catecholaminerg-induced early and delayed

70 afterdepolarizations (arrhythmia triggers) (Song et al., 1992), as well as the incidence of

71 ventricular fibrillation (Zuanetti et al., 1987; Collins and Billman, 1989). However, the

72 underlying mechanism of antiarrhythmic effect of M_2-receptor activation is not fully clarified.

73 Arrhythmias may develop when an arrhythmogenic substrate (e. g., dispersion of

74 repolarization) and arrhythmia triggers (e.g.: early and delayed afterdepolarizations)

75 simultaneously exist in the heart. The arrhythmogenic substrate could be prominent at

76 Purkinje–ventricle connection because of the relatively weak electrotonic coupling due to low

77 number of gap junctions (Varró and Baczkó, 2010). As a consequence of the different

78   pharmacological susceptibility of Purkinje fiber and ventricular muscle (Baláti et al, 1998),

79   the activation of $I_{K\text{-}ATP}$ may modulate the Purkinje and ventricular action potential duration

80   (APD) to different extents, and the developed APD dispersion may contribute to the onset of

81   arrhythmias.

82

83   The objective of this study was the investigation of the possible effect of acetylcholine on the

84    $I_{K\text{-}ATP}$ and on the $I_{K\text{-}ATP}$-mediated action potential dispersion under normal and hypoxic

85   conditions.

86

87   **Methods**

88   *Human tissues*

89   Non-diseased human hearts that were unusable for transplantation (based on logistical, not

90   patient-related considerations) were obtained from organ donors. Before cardiac explanation,

91   organ donor patients did not receive medication except dobutamine, furosemide and plasma

92   expanders. The investigations conform to the principles outlined in the *Declaration of*

93   *Helsinki* of the World Medical Association. All experimental protocols were approved by the

94   Scientific and Research Ethical Committee of the Medical Scientific Board at the Hungarian

95   Ministry of Health (ETT-TUKEB), under ethical approval No 4991-0/2010-1018EKU

96   (339/PI/010). Human cardiac tissue was stored in cardioplegic solution at 4°C for 4–8 hours.

97

98   *Animals*

99   All experiments using canine cardiac preparations were carried out in compliance with the

100   Guide for the Care and Use of Laboratory Animals (USA NIH publication NO 85-23, revised

101   1996) and conformed to the Directive 2010/63/EU of the European Parliament. The protocols

102   have been approved by the Ethical Committee for the Protection of Animals in Research of

103   the University of Szeged, Szeged, Hungary (approval number: I-74-24-2017) and by the

104   Department of Animal Health and Food Control of the Ministry of Agriculture and Rural

105   Development (authority approval number XIII/3331/2017).

106

107   *Conventional microelectrode technique*

108   Ventricular (papillary or trabecular) muscles were obtained from the right ventricle of canine

109   hearts. Free-running Purkinje fibers were identified as false tendons and isolated from both

110   ventricles of human and canine hearts. Canine hearts were removed through a right lateral

111   thoracotomy from anesthetized (thiopental 30 mg/kg i.v.) mongrel dogs of either sex

112   weighing 10–15 kg. At impalement, Purkinje fibers were observed under a surgical

113   microscope (Zeiss OPMI PRO). The preparations were placed in Locke's solution and

114   allowed to equilibrate for at least 2 hours while superfused (flow rate 4-5 ml/min) also with

115   Locke's solution containing (in mM): NaCl 120, KCl 4, $CaCl_2$ 2, $MgCl_2$ 1, $NaHCO_3$ 22, and

116   glucose 11. The pH of this solution was 7.40 to 7.45 when gassed with 95% O_2 and 5% CO_2

117   at 37 °C. In the experiments where the effects of tissue hypoxia were examined, we changed

118   the gas mixture to 95% N_2 and 5% CO_2, pH remained at 7.40 to 7.45. All experiments were

119   performed at 37 °C. During the equilibration period, preparations were stimulated at a basic

120   cycle length of 500 ms. Electrical pulses of 0.5–2 ms in duration at twice the diastolic

121   threshold in intensity (S_1) were delivered to the preparations through bipolar platinum

122   electrodes. Transmembrane potentials were recorded using glass capillary microelectrodes

123   filled with 3 M KCl (tip resistance: 5 to 15 MΩ). The microelectrodes were coupled through

124   an Ag-AgCl junction to the input of a high-impedance, capacitance-neutralizing amplifier

125   (Experimetria 2011). Intracellular recordings were displayed on a storage oscilloscope

126   (Hitachi V-555) and led to a computer system (APES) designed for on-line determination of

127   the following parameters: resting membrane potential, action potential amplitude, action

128   potential duration at 10% to 90% repolarization and the maximum rate of rise of the action

129   potential upstroke (V_{max}). Control recordings were obtained after equilibration period. The

130   compounds used in all experiments were purchased from Sigma/Merck.

131　*2.3. Cell isolation*

132　Ventricular myocytes were enzymatically dissociated from the left ventricle of dog hearts.

133　Canine hearts were removed through a right lateral thoracotomy from anesthetized (thiopental

134　30 mg/kg i.v.) mongrel dogs of either sex weighing 10–15 kg. Cardiac myocytes were isolated

135　from the left ventricle, containing an arterial branch through which the segment was perfused

136　on a Langendorff apparatus with solutions in the following sequence: normal Tyrode's

137　solution (containing in mM: 144 mM NaCl, 0.4 mM NaH_2PO_4, 4 mM KCl, 0.53 mM $MgSO_4$,

138　1.8 mM $CaCl_2$, 5.5 mM Glucose, 5 mM HEPES, pH 7.4 adjusted with NaOH) for 10 min,

139　Ca^{2+}-free Tyrode solution for 10 min and Ca^{2+}-free Tyrode solution containing collagenase

140　(Worthington type II, 0.66 mg/mL). To the final perfusion solution protease (type XIV, 0.12

141　mg/mL) was added at the 15 and the 30 minutes for digestion.

142

143　*2.4. Measurement of ionic currents*

144　One drop of cell suspension was placed in a transparent recording chamber mounted on the

145　stage of an inverted microscope (Olympus IX51, Tokyo, Japan), and individual myocytes

146　were allowed to settle and adhere to the chamber bottom for at least 5–10 min before

147　superfusion was initiated and maintained by gravity. Only rod-shaped cells with clear

148　striations were used. HEPES-buffered Tyrode's solution (composition in mM: NaCl 144,

149　NaH_2PO_4 0.4, KCl 4.0, $CaCl_2$ 1.8, $MgSO_4$ 0.53, glucose 5.5 and HEPES 5.0, at pH of 7.4)

150　was used as the normal superfusate. During the measurement of I_{K-ATP}, 1 μM nisoldipine was

151　added to the bath solution to block I_{CaL}, I_{Kr} was blocked by 0.1 μM dofetilide, and I_{Ks} was

152　blocked by 0.5 μM HMR-1556. Micropipettes were fabricated from borosilicate glass

153　capillaries (Science Products GmbH, Hofheim, Germany), using a P-97 Flaming/Brown

154　micropipette puller (Sutter Co, Novato, CA, USA), and had a resistance of 1.5–2.5 MΩ when

155　filled with pipette solution. The membrane currents were recorded with Axopatch-200B

156　amplifiers (Molecular Devices, Sunnyvale, CA, USA) by applying the whole-cell

157　configuration of the patch-clamp technique. The membrane currents were digitized with 250

158 kHz analogue to digital converters (Digidata 1440A, Molecular Devices, Sunnyvale, CA,

159 USA) under software control (pClamp 8 and pClamp 10, Molecular Devices, Sunnyvale, CA,

160 USA). The composition of the pipette solution (in mM) was the following: KOH 110, KCl

161 40, K_2ATP 5, $MgCl_2$ 5, EGTA 5, HEPES 10 and GTP 0.1 (pH was adjusted to 7.2 by aspartic

162 acid).

163

164 *2.5 Statistical analysis*

165 Results are expressed as mean ± S.E.M. Normality of distributions was verified using

166 Shapiro-Wilk test, and homogeneity of variances was verified using Bartlett's test in each

167 treatment group. Statistical comparisons were made using analysis of variance (ANOVA) for

168 repeated measurements, followed by Bonferroni's post-hoc test. Differences were considered

169 significant when $p < 0.05$.

170

171 **Results**

172 *1. Acetylcholine lengthened the APD after pinacidil-mediated action potential shortening*

173 Canine Purkinje fibers and ventricular papillary muscles were paced at 500 ms cycle length.

174 In canine Purkinje fibers (PFs; n=15), acetylcholine (5 μM) did not affect the repolarization

175 (233.6±4.7 to 231.7±4.6; Figures 1A and 1E). In contrast, in canine Purkinje fibers (n=8), the

176 I_{K-ATP} activator pinacidil, applied in 5 μM concentration, significantly abbreviated APD_{90}

177 (207.7±7.0 ms vs 113.1±9.1 ms, p<0.05) values. After steady state was reached, acetylcholine

178 was administered. Within 3 minutes, acetylcholine prolonged APD_{90} to 147.3±7.4 ms,

179 partially reversing the effects of pinacidil (Figures 1B and 1E; p<0.05).

180

181 Similarly, as observed in Purkinje fibers, 5 μM acetylcholine alone failed to influence the

182 APD of the ventricular muscle (APD_{90}: 172.6±5.7 ms vs 172.8±5.3 ms). Pinacidil (n=5;

183 5 μM) pretreatment significantly abbreviated the APD_{90} value (187.9±4.5 ms vs

184 163.7±6.4 ms, p<0.05), similarly to the effects observed in the case of PFs. After a period of

185   30 minutes, sufficient to reach a steady state, acetylcholine was added to the superfusate.

186   Within 4 minutes, acetylcholine (5 μM) prolonged APD_{90} to 172.1 ± 7.4 ms ($p<0.05$), thus

187   partially reversing the effects of pinacidil (Figures 1D and 1E).

188

189   *2. Acetylcholine decreased the calculated APD dispersion between PF and VM*

190   The changes in the difference between the APD_{90} values of PF and VM can be used to infer

191   the effects of pinacidil and acetylcholine on the dispersion between these cardiac tissue types

192   (Figure 2). The control APD_{90} dispersion (9.5%, 20 ms) was significantly increased upon

193   5 μM pinacidil application (44.7%, 51 ms). On the other hand, subsequently applied 5 μM

194   acetylcholine markedly decreased the repolarization heterogeneity (16.9%, 28 ms; $p<0.05$).

195

196   *3. Carbachol decreased the pinacidil-induced current activation*

197   During ionic current measurements, voltage ramps were used from a holding potential of

198   -90 mV. Membrane potential was hyperpolarized to -120 mV, and then was slowly (over 36 s)

199   depolarized to 60 mV. Ionic currents were analyzed and compared at 0 and +30 mV. We

200   found that carbachol did not change the control current when it was applied *without* pinacidil

201   (0 mV - control: 0.20 ± 0.2 pA/pF vs 3 μM carbachol: 0.32 ± 0.2 pA/pF, n=6 and +30 mV -

202   control: 0.55 ± 0.4 pA/pF vs 3 μM carbachol: 0.74 ± 0.3 pA/pF, n=6). In contrast, when 5 μM

203   pinacidil was applied first, subsequently employed carbachol significantly reduced the current

204   at both voltages (0 mV – control: 0.24 ± 0.2 pA/pF → 5 μM pinacidil: 2.03 ± 0.3 pA/pF → 3

205   μM carbachol: 1.51 ± 0.4 pA/pF, n=8, $p<0.05$. +30 mV - control: 0.78 ± 0.6 pA/pF → 5 μM

206   pinacidil: 3.17 ± 0.3 pA/pF → 3 μM carbachol: 2.26 ± 0.3 pA/pF, n=8, $p<0.05$).

207

208   These measurements were carried out with acetylcholine as well. However, we found

209   carbachol to be more stable during the applied long voltage protocol.

210

211   *4. Acetylcholine restored the APD after hypoxia-induced action potential shortening*

212   Simulated hypoxia, achieved by gassing the solution with N_2 and CO_2 instead of O_2 and CO_2,

213   resulted in a significant abbreviation of APD_{90} from 181.4 ± 5.7 ms to 135.0 ± 8.6 ms ($p<0.05$,

214   Figures 4A and 4B), and a decrease in amplitude (103.7 ± 2.8 mV vs 92 ± 3.5 mV). The

215   maximum rate of depolarization was also decreased (185.8 ± 15.8 V/s vs 156.1 ± 20.6 V/s).

216   When applied during hypoxia, 5 μM acetylcholine caused a significant APD_{90} prolongation to

217   164.4 ± 4.4 ms, partially reversing the effect of hypoxia on the repolarization. AMP returned to

218   a normal range (102.1 ± 1.6 mV), while V_{max} remained at 156.0 ± 16.1 V/s.

219

220   *5. Acetylcholine caused a slight abbreviation in human Purkinje fibers*

221   In human PFs (n=2), acetylcholine in 5 μM concentration caused a slight abbreviation of

222   APD_{90} from 269.0 ± 28.4 to 251.6 ± 42.85 ms   and   APD50   from 184.4 ± 20.0 ms   to

223   173.3 ± 27.1 ms without affecting other characteristics of the action potential (Figure 5).

224

225   **Discussion**

226   In this study we investigated the electrophysiological effects of muscarinic agonists on the

227   I_{K-ATP} current. We found that (i) under normal conditions acetylcholine did not influence the

228   action potential duration. (ii) In contrast, when I_{K-ATP} was pharmacologically activated by

229   pinacidil, subsequently applied acetylcholine lengthened the action potential duration as well

230   as (iii) reduced the pinacidil-induced ventricle-Purkinje APD dispersion. (iv) In line with this,

231   carbachol inhibited the I_{K-ATP} that was previously activated by pinacidil. (v) Acetylcholine

232   increased the APD after hypoxia-induced action potential shortening.

233

234   *Acetylcholine inhibits the I_{K-ATP} in canine ventricular myocytes*

235   It is well known that acetylcholine shortens the atrial APD and has been implicated in atrial

236   fibrillation (Nakayama et al, 1968). Acetylcholine directly affects the GIRK1/4 or

237   Kir3.1/Kir3.4 channels (Nobles et al, 2018; Corey and Clapham, 1998), encoded by *KCNJ3*

238 and *KCNJ4* genes (Kurachi, 1995). These channels are largely expressed in atrial, SA and AV

239 nodal cells (Galindo et al, 2016; Navarro-Polanco et al, 2013). At the same time, previous

240 studies (Terzic et al, 1994; Ito et al., 1994) claimed that acetylcholine activates the $I_{K\text{-ATP}}$

241 channels, even though the physiological consequences of this effect on the action potential

242 were not clarified.

243

244 The $I_{K\text{-ATP}}$ ATP-sensitive potassium channels comprise hetero-octamers consisting of four

245 inward rectifying potassium channel pore-forming subunits (Kir6.1 or Kir6.2, encoded by

246 *KCNJ8* and *KCNJ11* genes, respectively) and four ATP-binding cassette protein

247 sulphonylurea receptors (SUR1 or SUR2, encoded by *ABCC8* and *ABCC9* genes,

248 respectively; Inagaki et al, 195). An important feature of the $I_{K\text{-ATP}}$ is its closed state under

249 physiological intracellular ATP levels (i. e., under normoxia) and its activation by metabolic

250 stress, when the ratio of ATP/ADP is decreased, e. g., during myocardial ischemia (Deutsch et

251 al., 1991).

252

253 Activation of the sarcolemmal $I_{K\text{-ATP}}$ during myocardial ischemia shortens the action potential

254 of various cardiac tissues to different extents, thus it may promote APD dispersion and re-

255 entry type arrhythmias (Janse and Wit, 1989). Accordingly, several investigations found $I_{K\text{-}}$

256 $_{\text{ATP}}$ activation to be pro-arrhythmic (Chi et al., 1990), suggesting that sarcolemmal $I_{K\text{-ATP}}$

257 inhibition may prevent arrhythmias induced by myocardial ischemia and ischemia/reperfusion

258 (Billman et al, 1998; Englert et al, 2003; Vajda et al, 2007).

259

260 In our experiments under normal conditions, we found no effect of carbachol on the

261 membrane current (Figure 3) and, similarly, acetylcholine failed to influence the ventricular

262 and Purkinje APDs (Figures 1A and 1C). The observed discrepancy between our and previous

263 results, where an activation of $I_{K\text{-ATP}}$ was described upon acetylcholine administration (Terzic

264 et al, 1994; Ito et al, 1994; Kim et al., 1997), could be the consequence of the species

265 difference and the distinct experimental conditions.

266

267 In contrast, an important, and, to the best of our knowledge, previously not published result of

268 our study is that carbachol is able to suppress the pinacidil-activated I_{K-ATP}. As a consequence,

269 in parallel tissue action potential experiments, acetylcholine lengthened the APD as long as it

270 was previously shortened by the application of I_{K-ATP}-activator pinacidil. Since I_{K-ATP}

271 activation could be arrhythmogenic (Chi et al., 1990) by causing an increase in the APD

272 dispersion, this effect of acetylcholine raises the possibility of a novel antiarrhythmic

273 mechanism of the previously described antiarrhythmic effect of parasympathetic activation

274 during hypoxia (Song et al., 1992; Zuanetti et al., 1987; Collins and Billman, 1989).

275

276 Our experiments conducted under hypoxic conditions provided similar results (i. e.,

277 acetylcholine lengthened the hypoxia-induced shortened ventricular action potential;

278 Figure 4). Even though tissue hypoxia is a complex phenomenon (Carmeliet, 1999), during

279 which several factors change simultaneously (e. g., Ca^{2+}_i, Na^+_i, pH, conductance of gap

280 junctions, membrane potential etc.), it is feasible that I_{K-ATP} activation, as a response to ATP

281 depletion, is an important factor in the observed action potential shortening. Since

282 acetylcholine lengthened the action potential under hypoxic conditions, we suggest I_{K-ATP}

283 inhibition as a possible underlying mechanism.

284

285 *Acetylcholine decreased the pinacidil-induced ventricle–Purkinje APD dispersion*

286 Free-running Purkinje fibers connect to the ventricular muscle on a small surface area,

287 providing a relatively large-resistance coupling (Tranum-Jensen et al., 1991), and a large sink

288 for current flow that favors conduction blocks more than other parts of the healthy

289 myocardium. Also, due to the weaker electrotonic coupling, the dispersion of repolarization

290 here can be greater than in other areas (Martinez et al., 2018), causing the Purkinje–ventricle

291   APD ratio to have critical importance in arrhythmia generation. In our experiments, we found

292   significantly greater shortening in Purkinje fibers caused by pinacidil that could be the

293   consequence of the generally weaker repolarization reserve that makes the Purkinje action

294   potential to be more susceptible to any pharmacological interventions (Varró et al, 2000;

295   Baláti et al, 1998). Similarly, acetylcholine exerted larger lengthening in the Purkinje fiber

296   probably by the same reason that ultimately led to reduced ventricle–Purkinje APD

297   dispersion. The reduction of the ventricle–Purkinje fiber APD dispersion could suppress the

298   arrhythmogenic substrate providing a narrower vulnerable period for a critically timed

299   extrasystole to trigger a life-threatening arrhythmia under hypoxic conditions.

300

301   *Proposed mechanism*

302   Since inhibition of the K-ATP channels is possible by blocking various PKA-mediated

303   pathways (Tinker et al, 2018.), we suggest that the decrease of cAMP levels caused by the

304   activation of cardiac muscarinic receptors using acetylcholine/carbachol was the factor that

305   decreased the density of the I_{K-ATP} current in patch clamp measurements, leading to the

306   subsequent prolongation observed in action potential durations.

307

308   **Conclusions**

309   We found that muscarinic agonists inhibit the I_{K-ATP}. Therefore, during I_{K-ATP}-mediated action

310   potential shortening, acetylcholine causes asymmetrical action potential lengthening between

311   ventricular muscle and Purkinje fiber that leads to reduced APD dispersion.

312

313   These results suggest that the parasympathetic tone beyond suppressing the catecholaminerg-

314   induced arrhythmogenic triggers (Song et al., 1992) may be also able to reduce the

315   arrhythmogenic substrate under hypoxic conditions.

316

317

318   **Study Limitations**

319   (i) In our experiments, the ventricular and Purkinje fiber action potentials were measured

320   from electrically uncoupled tissue samples.

321   (ii) The presented effects were attributed to the M2 muscarinic receptor; nevertheless, the

322   exact level of contribution of other receptor subtypes was not addressed. To achieve this,

323   further studies are needed, utilizing specific agonist and antagonist drugs.

324

325   **Acknowledgments**

334 **References**

335 Baláti, B., Varró, A., & Papp, J. G. (1998). Comparison of the cellular electrophysiological characteristics of

336 canine left ventricular epicardium, M cells, endocardium and Purkinje fibers. *Acta Physiologica Scandinavica*,

337 *164*(2), 181–190. https://doi.org/10.1046/j.1365-201X.1998.00416.x

338

339 Billman, G. E., Englert, H. C., & Schölkens, B. A. (1998). HMR 1883, a novel cardioselective inhibitor of the

340 ATP-sensitive potassium channel. Part II: Effects on susceptibility to ventricular fibrillation induced by

341 myocardial ischemia in conscious dogs. *The Journal of Pharmacology and Experimental Therapeutics*, *286*(3),

342 1465–1473.

343

344 Carmeliet, E. (1999). Cardiac ionic currents and acute ischemia: From channels to arrhythmias. *Physiological*

345 *Reviews*, *79*(3), 917–1017. https://doi.org/10.1152/physrev.1999.79.3.917

346

347 Chi, L., Uprichard, A. C., & Lucchesi, B. R. (1990). Profibrillatory actions of pinacidil in a conscious canine

348 model of sudden coronary death. *Journal of Cardiovascular Pharmacology*, *15*(3), 452–464.

349 https://doi.org/10.1097/00005344-199003000-00016

350

351 Collins, M. N., & Billman, G. E. (1989). Autonomic response to coronary occlusion in animals susceptible to

352 ventricular fibrillation. *The American Journal of Physiology*, *257*(6 Pt 2), H1886-1894.

353 https://doi.org/10.1152/ajpheart.1989.257.6.H1886

354

355 Corey, S., & Clapham, D. E. (1998). Identification of native atrial G-protein-regulated inwardly rectifying K+

356 (GIRK4) channel homomultimers. *The Journal of Biological Chemistry*, *273*(42), 27499–27504.

357 https://doi.org/10.1074/jbc.273.42.27499

358

359 Deutsch, N., Klitzner, T. S., Lamp, S. T., & Weiss, J. N. (1991). Activation of cardiac ATP-sensitive K+ current

360 during hypoxia: Correlation with tissue ATP levels. *The American Journal of Physiology*, *261*(3 Pt 2), H671-

361 676. https://doi.org/10.1152/ajpheart.1991.261.3.H671

362

363 Englert, H. C., Heitsch, H., Gerlach, U., & Knieps, S. (2003). Blockers of the ATP-sensitive potassium channel

364 SUR2A/Kir6.2: A new approach to prevent sudden cardiac death. *Current Medicinal Chemistry. Cardiovascular*

365 *and Hematological Agents*, *1*(3), 253–271. https://doi.org/10.2174/1568016033477423

366

367 Harvey, R. D., & Belevych, A. E. (2003). Muscarinic regulation of cardiac ion channels. *British Journal of*

368 *Pharmacology*, *139*(6), 1074–1084. https://doi.org/10.1038/sj.bjp.0705338

369

370 Higgins, C. B., Vatner, S. F., & Braunwald, E. (1973). Parasympathetic control of the heart. *Pharmacological*

371 *Reviews*, *25*(1), 119–155.

372

373 Inagaki, N., Gonoi, T., Clement, J. P., Namba, N., Inazawa, J., Gonzalez, G., Aguilar-Bryan, L., Seino, S., &

374 Bryan, J. (1995). Reconstitution of IKATP: An inward rectifier subunit plus the sulfonylurea receptor. *Science*

375 *(New York, N.Y.)*, *270*(5239), 1166–1170. https://doi.org/10.1126/science.270.5239.1166

376

377 Ito, H., Vereecke, J., & Carmeliet, E. (1994). Mode of regulation by G protein of the ATP-sensitive K+ channel

378 in guinea-pig ventricular cell membrane. *The Journal of Physiology*, *478 (Pt 1)*, 101–107.

379 https://doi.org/10.1113/jphysiol.1994.sp020233

380

381 Janse, M. J., & Wit, A. L. (1989). Electrophysiological mechanisms of ventricular arrhythmias resulting from

382 myocardial ischemia and infarction. *Physiological Reviews*, *69*(4), 1049–1169.

383 https://doi.org/10.1152/physrev.1989.69.4.1049

384

385 Kim, D., Watson, M., & Indyk, V. (1997). ATP-dependent regulation of a G protein-coupled K+ channel

386 (GIRK1/GIRK4) expressed in oocytes. *The American Journal of Physiology*, *272*(1 Pt 2), H195-206.

387 https://doi.org/10.1152/ajpheart.1997.272.1.H195

388

389 Koumi, S., Wasserstrom, J. A., & Ten Eick, R. E. (1995). Beta-adrenergic and cholinergic modulation of the

390 inwardly rectifying K+ current in guinea-pig ventricular myocytes. *The Journal of Physiology*, *486 (Pt 3)*, 647–

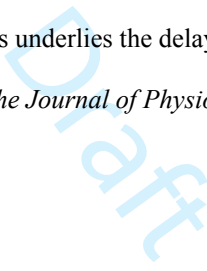391 659. https://doi.org/10.1113/jphysiol.1995.sp020841

392

393 Kurachi, Y. (1995). G protein regulation of cardiac muscarinic potassium channel. *The American Journal of*

394 *Physiology*, *269*(4 Pt 1), C821-830. https://doi.org/10.1152/ajpcell.1995.269.4.C821

395

396 Martinez, M. E., Walton, R. D., Bayer, J. D., Haïssaguerre, M., Vigmond, E. J., Hocini, M., & Bernus, O.

397 (2018). Role of the Purkinje-Muscle Junction on the Ventricular Repolarization Heterogeneity in the Healthy and

398   Ischemic Ovine Ventricular Myocardium. *Frontiers in Physiology*, *9*, 718.

399   https://doi.org/10.3389/fphys.2018.00718

400

401   Nagy, N., Szél, T., Jost, N., Tóth, A., Gy. Papp, J., & Varró, A. (2015). Novel experimental results in human

402   cardiac electrophysiology: Measurement of the Purkinje fibre action potential from the undiseased human heart.

403   *Canadian Journal of Physiology and Pharmacology*, *93*(9), 803–810. https://doi.org/10.1139/cjpp-2014-0532

404

405   Nakayama, K., Suzuki, Y., & Hashimoto, K. (1968). Sustained atrial fibrillation by acetylcholine infusion into

406   the sinus node artery. *The Tohoku Journal of Experimental Medicine*, *96*(4), 333–339.

407   https://doi.org/10.1620/tjem.96.333

408

409   Navarro-Polanco, R. A., Aréchiga-Figueroa, I. A., Salazar-Fajardo, P. D., Benavides-Haro, D. E., Rodríguez-

410   Elías, J. C., Sachse, F. B., Tristani-Firouzi, M., Sánchez-Chapula, J. A., & Moreno-Galindo, E. G. (2013).

411   Voltage sensitivity of M2 muscarinic receptors underlies the delayed rectifier-like activation of ACh-gated K(+)

412   current by choline in feline atrial myocytes. *The Journal of Physiology*, *591*(17), 4273–4286.

413   https://doi.org/10.1113/jphysiol.2013.255166

414

415   Nobles, M., Montaigne, D., Sebastian, S., Birnbaumer, L., & Tinker, A. (2018). Differential effects of inhibitory

416   G protein isoforms on G protein-gated inwardly rectifying K+ currents in adult murine atria. *American Journal*

417   *of Physiology. Cell Physiology*, *314*(5), C616–C626. https://doi.org/10.1152/ajpcell.00271.2016

418

419   Pappano, A. J., & Carmeliet, E. E. (1979). Epinephrine and the pacemaking mechanism at plateau potentials in

420   sheep cardiac Purkinje fibers. *Pflugers Archiv: European Journal of Physiology*, *382*(1), 17–26.

421   https://doi.org/10.1007/BF00585899

422

423   Recordati, G., Schwartz, P. J., Pagani, M., Malliani, A., & Brown, A. M. (1971). Activation of cardiac vagal

424   receptors during myocardial ischemia. *Experientia*, *27*(12), 1423–1424. https://doi.org/10.1007/BF02154267

425

426   Song, Y., Thedford, S., Lerman, B. B., & Belardinelli, L. (1992). Adenosine-sensitive afterdepolarizations and

427   triggered activity in guinea pig ventricular myocytes. *Circulation Research*, *70*(4), 743–753.

428   https://doi.org/10.1161/01.res.70.4.743

429

430 Terzic, A., Tung, R. T., Inanobe, A., Katada, T., & Kurachi, Y. (1994). G proteins activate ATP-sensitive K+

431 channels by antagonizing ATP-dependent gating. *Neuron*, *12*(4), 885–893. https://doi.org/10.1016/0896-

432 6273(94)90340-9

433

434 Tranum-Jensen, J., Wilde, A. A., Vermeulen, J. T., & Janse, M. J. (1991). Morphology of electrophysiologically

435 identified junctions between Purkinje fibers and ventricular muscle in rabbit and pig hearts. *Circulation*

436 *Research*, *69*(2), 429–437. https://doi.org/10.1161/01.res.69.2.429

437

438 Vajda, S., Baczkó, I., & Leprán, I. (2007). Selective cardiac plasma-membrane K(ATP) channel inhibition is

439 defibrillatory and improves survival during acute myocardial ischemia and reperfusion. *European Journal of*

440 *Pharmacology*, *577*(1–3), 115–123. https://doi.org/10.1016/j.ejphar.2007.08.016

441

442 Varró, A., & Baczkó, I. (2010). Possible mechanisms of sudden cardiac death in top athletes: A basic cardiac

443 electrophysiological point of view. *Pflugers Archiv: European Journal of Physiology*, *460*(1), 31–40.

444 https://doi.org/10.1007/s00424-010-0798-0

445

446 Varro, A., Baláti, B., Iost, N., Takács, J., Virág, L., Lathrop, D. A., Csaba, L., Tálosi, L., & Papp, J. G. (2000).

447 The role of the delayed rectifier component IKs in dog ventricular muscle and Purkinje fibre repolarization. *The*

448 *Journal of Physiology*, *523 Pt 1*, 67–81. https://doi.org/10.1111/j.1469-7793.2000.00067.x

449

450 Weiss, J. N., & Venkatesh, N. (1993). Metabolic regulation of cardiac ATP-sensitive K+ channels.

451 *Cardiovascular Drugs and Therapy*, *7 Suppl 3*, 499–505. https://doi.org/10.1007/BF00877614

452

453 Zuanetti, G., De Ferrari, G. M., Priori, S. G., & Schwartz, P. J. (1987). Protective effect of vagal stimulation on

454 reperfusion arrhythmias in cats. *Circulation Research*, *61*(3), 429–435. https://doi.org/10.1161/01.res.61.3.429

455   **Figure Legends**

456   **Figure 1.** Representative traces of Purkinje fiber (A, B) and ventricular muscle preparations

457   (C, D); 5 μM acetylcholine (red dotted lines) alone caused no changes in either preparation

458   type (A, C), while it caused significant prolongation when applied cummulatively after 5 μM

459   pinacidil (B, D, pinacidil effect represented as blue dashed lines). Bars in panel E represent

460   the values of APD_{90} in each treatment group, from top to bottom corresponding to the traces

461   A to D. Abbreviations under bars: C, control; P, pinacidil, A, acetylcholine. The pacing cycle

462   length was 500 ms. Values are mean ± SEM; *,# $p<0.05$ RM-ANOVA followed by

463   Bonferroni's post-hoc test.

464

465   **Figure 2.** Pinacidil (5 μM) increased the action potential duration dispersion (indicated by

466   ΔAPD_{90} in percentages, and in ms above the bars) between Purkinje fiber and ventricular

467   muscle preparations, while acetylcholine (5 μM), when applied after pinacidil, decreased

468   dispersion. The pacing cycle length was 500 ms.

469

470   **Figure 3.** Effect of carbachol on $I_{K\text{-}ATP}$. Ionic currents were measured under a slow voltage

471   ramp protocol (panel A) between -120 mV and 60 mV. The currents were analysed at 0 and

472   30 mV. Panel B demonstrates original representative current traces (left) and bar graphs

473   (right) where 3 μM carbachol (dotted line) failed to influence the control current analysed at

474   0 mV. Inset shows identical current fractions between –3 mV and 45 mV (indicated by dashed

475   rectangle). Current traces in panel C as well as in the inset, illustrate large increase of the

476   membrane current after application of 5 μM pinacidil (blue dashed line) that was inhibited by

477   the subsequently applied 3 μM carbachol (red dotted line). In bar graphs (right), asterisk

478   denotes significant change between control (left column) and pinacidil (middle column),

479   while hash tag indicates significant change between pinacidil (middle column) and carbachol

480   (right column).

481

482   **Figure 4.** Representative action potential trace (A) showing that hypoxic conditions caused

483   significant action potential duration abbreviation and decreased mean diastolic potential and

484   amplitude in canine ventricular preparations (blue dashed line), while acetylcholine (5 μM)

485   caused a significant prolongation in action potential duration (red dotted line). Values of

486   APD_{90} are represented as bars (B). Abbreviations under bars: C, control; H, hypoxia, A,

487   acetylcholine. The pacing cycle length was 500 ms. Values are mean ± SEM; *,#$p<0.05$,

488   RM-ANOVA followed by Bonferroni's post-hoc test.

489

490   **Figure 5.** Representative action potential showing the effect of acetylcholine (5 μM, red

491   dotted line) on a Purkinje fiber taken from a human donor heart (A). Values of APD_{90} are

492   represented as bars (B). Abbreviations under bars: C, control; A, acetylcholine. The pacing

493   cycle length was 500 ms. Values are mean ± SEM.

1　**Muscarinic agonists inhibit the ATP-dependent potassium current and suppress the**

2　**ventricle-Purkinje action potential dispersion**

3

4　Tibor Magyar[a,§], Tamás Árpádffy-Lovas[a,§], Bence Pászti[a], Noémi Tóth[a], Jozefina Szlovák[a],

5　Péter Gazdag[a], Zsófia Kohajda[b], András Gyökeres[a], Balázs Györe[d], Zsolt Gurabi[a], Norbert

6　Jost[a,b,c], László Virág[a,c], Julius Gy. Papp[a,b], Norbert Nagy[a,b,#], István Koncz[a,*, #]

7

8

9　[a]Department of Pharmacology and Pharmacotherapy, Faculty of Medicine, University of

10　Szeged, Szeged, Hungary;

11　[b]MTA-SZTE Research Group of Cardiovascular Pharmacology, Hungarian Academy of

12　Sciences, Szeged, Hungary

13　[c]Department of Pharmacology and Pharmacotherapy, Interdisciplinary Excellence Centre,

14　University of Szeged, Szeged, Hungary

15　[d]Faculty of Dentistry, University of Szeged, Hungary

16

17　[§] Shared first authorship

18　[#] Shared senior authorship

19

20　*Author for correspondence at:

21　István Koncz MD, PhD

22　Department of Pharmacology & Pharmacotherapy

23　Faculty of Medicine

24　University of Szeged

25　Dóm tér 12,

26　H-6720 Szeged, Hungary

27　E-mail: koncz.istvan@med.u-szeged.hu

28   **Abstract**

29   **Introduction:** Activation of the parasympathetic nervous system has been reported to have an

30   antiarrhythmic role during ischemia-reperfusion injury by decreasing the arrhythmia triggers.

31   Furthermore, it was reported that the parasympathetic neurotransmitter acetylcholine is able to

32   modulate the ATP-dependent K-current (I_{K-ATP}), a crucial current activated during hypoxia.

33   However, the possible significance of this current modulation in the antiarrhythmic

34   mechanism is not fully clarified.

35   **Methods:** Action potentials were measured using the conventional microelectrode technique

36   from canine left ventricular papillary muscle and free-running Purkinje fibers, under normal

37   and hypoxic conditions. Ionic currents were measured using the whole-cell configuration of

38   the patch clamp method.

39   **Results:** 5 μM acetylcholine did not influence the action potential duration (APD) either in

40   Purkinje fibers or in papillary muscle preparations. In contrast, it significantly lengthened the

41   APD and suppressed the Purkinje–ventricle APD dispersion when it was administered after

42   5 μM pinacidil application. 3 μM carbachol reduced the pinacidil-activated I_{K-ATP} under

43   voltage-clamp condition. Acetylcholine lengthened the ventricular action potential under

44   simulated ischemia condition.

45   **Conclusion:** In this study we found that acetylcholine inhibits the I_{K-ATP} and thus suppresses

46   the ventricle-Purkinje APD dispersion. We conclude that parasympathetic tone may reduce

47   the arrhythmogenic substrate exerting a complex antiarrhythmic mechanism during hypoxic

48   conditions.

49

50   *Key words:* acetylcholine, Purkinje fibers, papillary muscles, hypoxia

Introduction

The parasympathetic nervous system has a crucial role in controlling the actual heart rate and impulse propagation via influencing the sinoatrial and atrioventricular nodes (Higgins et al., 1973). The parasympathetic nerve endings operate by releasing acetylcholine that acts on M_2-receptors, activating several intracellular signaling routes, and ultimately influencing the cardiac ion channels (Harvey and Belevych, 2003). Even though the parasympathetic nervous system primarily innervates the supraventricular areas of the heart, there are certain important ion channels in the ventricular muscle that are known to be influenced by the release of acetylcholine. It has been previously reported that the inward rectifier potassium current (I_{K1}; Koumi et al., 1995) and the slow component of the delayed rectifier (I_{Ks}; Pappano and Carmeliet, 1979) are inhibited, whereas $I_{K\text{-ATP}}$ and $I_{K\text{-ACh}}$ are activated by acetylcholine via G proteins (Terzic et al, 1994; Ito et al., 1994; Kim et al., 1997).

The importance of these effects of acetylcholine is underpinned by the fact that the activation of $I_{K\text{-ATP}}$ channels is well known during hypoxia/ischemia, in which situations the duration of the action potential is shortened (Weiss and Venkatesh, 1993). Furthermore, it was reported that vagal activation is also facilitated under ischemia–reperfusion (Recordati et al., 1971). This vagal activation during hypoxia could be antiarrhythmic, since it was reported that increased parasympathetic tone reduces the catecholaminerg-induced early and delayed afterdepolarizations (arrhythmia triggers) (Song et al., 1992), as well as the incidence of ventricular fibrillation (Zuanetti et al., 1987; Collins and Billman, 1989). However, the underlying mechanism of antiarrhythmic effect of M_2-receptor activation is not fully clarified. Arrhythmias may develop when an arrhythmogenic substrate (e. g., dispersion of repolarization) and arrhythmia triggers (e.g.: early and delayed afterdepolarizations) simultaneously exist in the heart. The arrhythmogenic substrate could be prominent at Purkinje–ventricle connection because of the relatively weak electrotonic coupling due to low number of gap junctions (Varró and Baczkó, 2010). As a consequence of the different

78   pharmacological susceptibility of Purkinje fiber and ventricular muscle (Baláti et al, 1998),

79   the activation of $I_{K\text{-}ATP}$ may modulate the Purkinje and ventricular action potential duration

80   (APD) to different extents, and the developed APD dispersion may contribute to the onset of

81   arrhythmias.

82

83   The objective of this study was the investigation of the possible effect of acetylcholine on the

84   $I_{K\text{-}ATP}$ and on the $I_{K\text{-}ATP}$-mediated action potential dispersion under normal and hypoxic

85   conditions.

86

87   **Methods**

88   *Human tissues*

89   Non-diseased human hearts that were unusable for transplantation (based on logistical, not

90   patient-related considerations) were obtained from organ donors. Before cardiac explanation,

91   organ donor patients did not receive medication except dobutamine, furosemide and plasma

92   expanders. The investigations conform to the principles outlined in the *Declaration of*

93   *Helsinki* of the World Medical Association. All experimental protocols were approved by the

94   Scientific and Research Ethical Committee of the Medical Scientific Board at the Hungarian

95   Ministry of Health (ETT-TUKEB), under ethical approval No 4991-0/2010-1018EKU

96   (339/PI/010). Human cardiac tissue was stored in cardioplegic solution at 4°C for 4–8 hours.

97

98   *Animals*

99   All experiments using canine cardiac preparations were carried out in compliance with the

100   Guide for the Care and Use of Laboratory Animals (USA NIH publication NO 85-23, revised

101   1996) and conformed to the Directive 2010/63/EU of the European Parliament. The protocols

102   have been approved by the Ethical Committee for the Protection of Animals in Research of

103   the University of Szeged, Szeged, Hungary (approval number: I-74-24-2017) and by the

104   Department of Animal Health and Food Control of the Ministry of Agriculture and Rural

105   Development (authority approval number XIII/3331/2017).

106

107   *Conventional microelectrode technique*

108   Ventricular (papillary or trabecular) muscles were obtained from the right ventricle of canine

109   hearts. Free-running Purkinje fibers were identified as false tendons and isolated from both

110   ventricles of human and canine hearts. Canine hearts were removed through a right lateral

111   thoracotomy from anesthetized (thiopental 30 mg/kg i.v.) mongrel dogs of either sex

112   weighing 10–15 kg. At impalement, Purkinje fibers were observed under a surgical

113   microscope (Zeiss OPMI PRO). The preparations were placed in Locke's solution and

114   allowed to equilibrate for at least 2 hours while superfused (flow rate 4-5 ml/min) also with

115   Locke's solution containing (in mM): NaCl 120, KCl 4, $CaCl_2$ 2, $MgCl_2$ 1, $NaHCO_3$ 22, and

116   glucose 11. The pH of this solution was 7.40 to 7.45 when gassed with 95% O_2 and 5% CO_2

117   at 37 °C. In the experiments where the effects of tissue hypoxia were examined, we changed

118   the gas mixture to 95% N_2 and 5% CO_2, pH remained at 7.40 to 7.45. All experiments were

119   performed at 37 °C. During the equilibration period, preparations were stimulated at a basic

120   cycle length of 500 ms. Electrical pulses of 0.5–2 ms in duration at twice the diastolic

121   threshold in intensity (S_1) were delivered to the preparations through bipolar platinum

122   electrodes. Transmembrane potentials were recorded using glass capillary microelectrodes

123   filled with 3 M KCl (tip resistance: 5 to 15 MΩ). The microelectrodes were coupled through

124   an Ag-AgCl junction to the input of a high-impedance, capacitance-neutralizing amplifier

125   (Experimetria 2011). Intracellular recordings were displayed on a storage oscilloscope

126   (Hitachi V-555) and led to a computer system (APES) designed for on-line determination of

127   the following parameters: resting membrane potential, action potential amplitude, action

128   potential duration at 10% to 90% repolarization and the maximum rate of rise of the action

129   potential upstroke (V_{max}). Control recordings were obtained after equilibration period. The

130   compounds used in all experiments were purchased from Sigma/Merck.

131 *2.3. Cell isolation*

132 Ventricular myocytes were enzymatically dissociated from the left ventricle of dog hearts.

133 Canine hearts were removed through a right lateral thoracotomy from anesthetized (thiopental

134 30 mg/kg i.v.) mongrel dogs of either sex weighing 10–15 kg. Cardiac myocytes were isolated

135 from the left ventricle, containing an arterial branch through which the segment was perfused

136 on a Langendorff apparatus with solutions in the following sequence: normal Tyrode's

137 solution (containing in mM: 144 mM NaCl, 0.4 mM NaH_2PO_4, 4 mM KCl, 0.53 mM $MgSO_4$,

138 1.8 mM $CaCl_2$, 5.5 mM Glucose, 5 mM HEPES, pH 7.4 adjusted with NaOH) for 10 min,

139 Ca^{2+}-free Tyrode solution for 10 min and Ca^{2+}-free Tyrode solution containing collagenase

140 (Worthington type II, 0.66 mg/mL). To the final perfusion solution protease (type XIV, 0.12

141 mg/mL) was added at the 15 and the 30 minutes for digestion.

142

143 *2.4. Measurement of ionic currents*

144 One drop of cell suspension was placed in a transparent recording chamber mounted on the

145 stage of an inverted microscope (Olympus IX51, Tokyo, Japan), and individual myocytes

146 were allowed to settle and adhere to the chamber bottom for at least 5–10 min before

147 superfusion was initiated and maintained by gravity. Only rod-shaped cells with clear

148 striations were used. HEPES-buffered Tyrode's solution (composition in mM: NaCl 144,

149 NaH_2PO_4 0.4, KCl 4.0, $CaCl_2$ 1.8, $MgSO_4$ 0.53, glucose 5.5 and HEPES 5.0, at pH of 7.4)

150 was used as the normal superfusate. During the measurement of I_{K-ATP}, 1 μM nisoldipine was

151 added to the bath solution to block $I_{CaL,}$ I_{Kr} was blocked by 0.1 μM dofetilide, and I_{Ks} was

152 blocked by 0.5 μM HMR-1556. Micropipettes were fabricated from borosilicate glass

153 capillaries (Science Products GmbH, Hofheim, Germany), using a P-97 Flaming/Brown

154 micropipette puller (Sutter Co, Novato, CA, USA), and had a resistance of 1.5–2.5 MΩ when

155 filled with pipette solution. The membrane currents were recorded with Axopatch-200B

156 amplifiers (Molecular Devices, Sunnyvale, CA, USA) by applying the whole-cell

157 configuration of the patch-clamp technique. The membrane currents were digitized with 250

158   kHz analogue to digital converters (Digidata 1440A, Molecular Devices, Sunnyvale, CA,

159   USA) under software control (pClamp 8 and pClamp 10, Molecular Devices, Sunnyvale, CA,

160   USA). The composition of the pipette solution (in mM) was the following: KOH 110, KCl

161   40, K_2ATP 5, $MgCl_2$ 5, EGTA 5, HEPES 10 and GTP 0.1 (pH was adjusted to 7.2 by aspartic

162   acid).

163

164   *2.5 Statistical analysis*

165   Results are expressed as mean ± S.E.M. Normality of distributions was verified using

166   Shapiro-Wilk test, and homogeneity of variances was verified using Bartlett's test in each

167   treatment group. Statistical comparisons were made using analysis of variance (ANOVA) for

168   repeated measurements, followed by Bonferroni's post-hoc test. Differences were considered

169   significant when $p < 0.05$.

170

171   **Results**

172   *1. Acetylcholine lengthened the APD after pinacidil-mediated action potential shortening*

173   Canine Purkinje fibers and ventricular papillary muscles were paced at 500 ms cycle length.

174   In canine Purkinje fibers (PFs; n=15), acetylcholine (5 μM) did not affect the repolarization

175   (233.6±4.7 to 231.7±4.6; Figures 1A and 1E). In contrast, in canine Purkinje fibers (n=8), the

176   I_{K-ATP} activator pinacidil, applied in 5 μM concentration, significantly abbreviated APD_{90}

177   (207.7±7.0 ms vs 113.1±9.1 ms, p<0.05) values. After steady state was reached, acetylcholine

178   was administered. Within 3 minutes, acetylcholine prolonged APD_{90} to 147.3±7.4 ms,

179   partially reversing the effects of pinacidil (Figures 1B and 1E; p<0.05).

180

181   Similarly, as observed in Purkinje fibers, 5 μM acetylcholine alone failed to influence the

182   APD of the ventricular muscle (APD_{90}: 172.6±5.7 ms vs 172.8±5.3 ms). Pinacidil (n=5;

183   5 μM) pretreatment significantly abbreviated the APD_{90} value (187.9±4.5 ms vs

184   163.7±6.4 ms, p<0.05), similarly to the effects observed in the case of PFs. After a period of

185 30 minutes, sufficient to reach a steady state, acetylcholine was added to the superfusate.

186 Within 4 minutes, acetylcholine (5 μM) prolonged APD_{90} to 172.1±7.4 ms (p<0.05), thus

187 partially reversing the effects of pinacidil (Figures 1D and 1E).

188

189 *2. Acetylcholine decreased the calculated APD dispersion between PF and VM*

190 The changes in the difference between the APD_{90} values of PF and VM can be used to infer

191 the effects of pinacidil and acetylcholine on the dispersion between these cardiac tissue types

192 (Figure 2). The control APD_{90} dispersion (9.5%, 20 ms) was significantly increased upon

193 5 μM pinacidil application (44.7%, 51 ms). On the other hand, subsequently applied 5 μM

194 acetylcholine markedly decreased the repolarization heterogeneity (16.9%, 28 ms; p<0.05).

195

196 *3. Carbachol decreased the pinacidil-induced current activation*

197 During ionic current measurements, voltage ramps were used from a holding potential of

198 -90 mV. Membrane potential was hyperpolarized to -120 mV, and then was slowly (over 36 s)

199 depolarized to 60 mV. Ionic currents were analyzed and compared at 0 and +30 mV. We

200 found that carbachol did not change the control current when it was applied *without* pinacidil

201 (0 mV - control: 0.20±0.2 pA/pF vs 3 μM carbachol: 0.32±0.2 pA/pF, n=6 and +30 mV -

202 control: 0.55±0.4 pA/pF vs 3 μM carbachol: 0.74±0.3 pA/pF, n=6). In contrast, when 5 μM

203 pinacidil was applied first, subsequently employed carbachol significantly reduced the current

204 at both voltages (0 mV – control: 0.24±0.2 pA/pF → 5 μM pinacidil: 2.03±0.3 pA/pF → 3

205 μM carbachol: 1.51±0.4 pA/pF, n=8, p<0.05. +30 mV - control: 0.78±0.6 pA/pF → 5 μM

206 pinacidil: 3.17±0.3 pA/pF → 3 μM carbachol: 2.26±0.3 pA/pF, n=8, p<0.05).

207

208 These measurements were carried out with acetylcholine as well. However, we found

209 carbachol to be more stable during the applied long voltage protocol.

210

211　*4. Acetylcholine restored the APD after hypoxia-induced action potential shortening*

212　Simulated hypoxia, achieved by gassing the solution with N_2 and CO_2 instead of O_2 and CO_2,

213　resulted in a significant abbreviation of APD_{90} from 181.4 ± 5.7 ms to 135.0 ± 8.6 ms (p<0.05,

214　Figures 4A and 4B), and a decrease in amplitude (103.7 ± 2.8 mV vs 92 ± 3.5 mV). The

215　maximum rate of depolarization was also decreased (185.8 ± 15.8 V/s vs 156.1 ± 20.6 V/s).

216　When applied during hypoxia, 5 μM acetylcholine caused a significant APD_{90} prolongation to

217　164.4 ± 4.4 ms, partially reversing the effect of hypoxia on the repolarization. AMP returned to

218　a normal range (102.1 ± 1.6 mV), while V_{max} remained at 156.0 ± 16.1 V/s.

219

220　*5. Acetylcholine caused a slight abbreviation in human Purkinje fibers*

221　In human PFs (n=2), acetylcholine in 5 μM concentration caused a slight abbreviation of

222　APD_{90}　from　269.0 ± 28.4 to　251.6 ± 42.85 ms　and　APD50　from　184.4 ± 20.0 ms　to

223　173.3 ± 27.1 ms without affecting other characteristics of the action potential (Figure 5).

224

225　**Discussion**

226　In this study we investigated the electrophysiological effects of muscarinic agonists on the

227　$I_{K\text{-}ATP}$ current. We found that (i) under normal conditions acetylcholine did not influence the

228　action potential duration. (ii) In contrast, when $I_{K\text{-}ATP}$ was pharmacologically activated by

229　pinacidil, subsequently applied acetylcholine lengthened the action potential duration as well

230　as (iii) reduced the pinacidil-induced ventricle-Purkinje APD dispersion. (iv) In line with this,

231　carbachol inhibited the $I_{K\text{-}ATP}$ that was previously activated by pinacidil. (v) Acetylcholine

232　increased the APD after hypoxia-induced action potential shortening.

233

234　*Acetylcholine inhibits the $I_{K\text{-}ATP}$ in canine ventricular myocytes*

235　It is well known that acetylcholine shortens the atrial APD and has been implicated in atrial

236　fibrillation (Nakayama et al, 1968). Acetylcholine directly affects the GIRK1/4 or

237　Kir3.1/Kir3.4 channels (Nobles et al, 2018; Corey and Clapham, 1998), encoded by *KCNJ3*

238   and *KCNJ4* genes (Kurachi, 1995). These channels are largely expressed in atrial, SA and AV

239   nodal cells (Galindo et al, 2016; Navarro-Polanco et al, 2013). At the same time, previous

240   studies (Terzic et al, 1994; Ito et al., 1994) claimed that acetylcholine activates the I_{K-ATP}

241   channels, even though the physiological consequences of this effect on the action potential

242   were not clarified.

243

244   The I_{K-ATP} ATP-sensitive potassium channels comprise hetero-octamers consisting of four

245   inward rectifying potassium channel pore-forming subunits (Kir6.1 or Kir6.2, encoded by

246   *KCNJ8* and *KCNJ11* genes, respectively) and four ATP-binding cassette protein

247   sulphonylurea receptors (SUR1 or SUR2, encoded by *ABCC8* and *ABCC9* genes,

248   respectively; Inagaki et al, 195). An important feature of the I_{K-ATP} is its closed state under

249   physiological intracellular ATP levels (i. e., under normoxia) and its activation by metabolic

250   stress, when the ratio of ATP/ADP is decreased, e. g., during myocardial ischemia (Deutsch et

251   al., 1991).

252

253   Activation of the sarcolemmal I_{K-ATP} during myocardial ischemia shortens the action potential

254   of various cardiac tissues to different extents, thus it may promote APD dispersion and re-

255   entry type arrhythmias (Janse and Wit, 1989). Accordingly, several investigations found I_{K-ATP}

256   activation to be pro-arrhythmic (Chi et al., 1990), suggesting that sarcolemmal I_{K-ATP}

257   inhibition may prevent arrhythmias induced by myocardial ischemia and ischemia/reperfusion

258   (Billman et al, 1998; Englert et al, 2003; Vajda et al, 2007).

259

260   In our experiments under normal conditions, we found no effect of carbachol on the

261   membrane current (Figure 3) and, similarly, acetylcholine failed to influence the ventricular

262   and Purkinje APDs (Figures 1A and 1C). The observed discrepancy between our and previous

263   results, where an activation of I_{K-ATP} was described upon acetylcholine administration (Terzic

264   et al, 1994; Ito et al, 1994; Kim et al., 1997), could be the consequence of the species

265   difference and the distinct experimental conditions.

266

267   In contrast, an important, and, to the best of our knowledge, previously not published result of

268   our study is that carbachol is able to suppress the pinacidil-activated I_{K-ATP}. As a consequence,

269   in parallel tissue action potential experiments, acetylcholine lengthened the APD as long as it

270   was previously shortened by the application of I_{K-ATP}-activator pinacidil. Since I_{K-ATP}

271   activation could be arrhythmogenic (Chi et al., 1990) by causing an increase in the APD

272   dispersion, this effect of acetylcholine raises the possibility of a novel antiarrhythmic

273   mechanism of the previously described antiarrhythmic effect of parasympathetic activation

274   during hypoxia (Song et al., 1992; Zuanetti et al., 1987; Collins and Billman, 1989).

275

276   Our experiments conducted under hypoxic conditions provided similar results (i. e.,

277   acetylcholine lengthened the hypoxia-induced shortened ventricular action potential;

278   Figure 4). Even though tissue hypoxia is a complex phenomenon (Carmeliet, 1999), during

279   which several factors change simultaneously (e. g., Ca^{2+}_i, Na^+_i, pH, conductance of gap

280   junctions, membrane potential etc.), it is feasible that I_{K-ATP} activation, as a response to ATP

281   depletion, is an important factor in the observed action potential shortening. Since

282   acetylcholine lengthened the action potential under hypoxic conditions, we suggest I_{K-ATP}

283   inhibition as a possible underlying mechanism.

284

285   *Acetylcholine decreased the pinacidil-induced ventricle–Purkinje APD dispersion*

286   Free-running Purkinje fibers connect to the ventricular muscle on a small surface area,

287   providing a relatively large-resistance coupling (Tranum-Jensen et al., 1991), and a large sink

288   for current flow that favors conduction blocks more than other parts of the healthy

289   myocardium. Also, due to the weaker electrotonic coupling, the dispersion of repolarization

290   here can be greater than in other areas (Martinez et al., 2018), causing the Purkinje–ventricle

291 APD ratio to have critical importance in arrhythmia generation. In our experiments, we found

292 significantly greater shortening in Purkinje fibers caused by pinacidil that could be the

293 consequence of the generally weaker repolarization reserve that makes the Purkinje action

294 potential to be more susceptible to any pharmacological interventions (Varró et al, 2000;

295 Baláti et al, 1998). Similarly, acetylcholine exerted larger lengthening in the Purkinje fiber

296 probably by the same reason that ultimately led to reduced ventricle–Purkinje APD

297 dispersion. The reduction of the ventricle–Purkinje fiber APD dispersion could suppress the

298 arrhythmogenic substrate providing a narrower vulnerable period for a critically timed

299 extrasystole to trigger a life-threatening arrhythmia under hypoxic conditions.

300

301 *Proposed mechanism*

302 Since inhibition of the K-ATP channels is possible by blocking various PKA-mediated

303 pathways (Tinker et al, 2018.), we suggest that the decrease of cAMP levels caused by the

304 activation of cardiac muscarinic receptors using acetylcholine/carbachol was the factor that

305 decreased the density of the $I_{K\text{-}ATP}$ current in patch clamp measurements, leading to the

306 subsequent prolongation observed in action potential durations.

307

308 **Conclusions**

309 We found that muscarinic agonists inhibit the $I_{K\text{-}ATP}$. Therefore, during $I_{K\text{-}ATP}$-mediated action

310 potential shortening, acetylcholine causes asymmetrical action potential lengthening between

311 ventricular muscle and Purkinje fiber that leads to reduced APD dispersion.

312

313 These results suggest that the parasympathetic tone beyond suppressing the catecholaminerg-

314 induced arrhythmogenic triggers (Song et al., 1992) may be also able to reduce the

315 arrhythmogenic substrate under hypoxic conditions.

316

317

318   **Study Limitations**

319   (i) In our experiments, the ventricular and Purkinje fiber action potentials were measured

320   from electrically uncoupled tissue samples.

321   (ii) The presented effects were attributed to the M2 muscarinic receptor; nevertheless, the

322   exact level of contribution of other receptor subtypes was not addressed. To achieve this,

323   further studies are needed, utilizing specific agonist and antagonist drugs.

324

325   **Acknowledgments**

References

Baláti, B., Varró, A., & Papp, J. G. (1998). Comparison of the cellular electrophysiological characteristics of canine left ventricular epicardium, M cells, endocardium and Purkinje fibers. *Acta Physiologica Scandinavica*, *164*(2), 181–190. https://doi.org/10.1046/j.1365-201X.1998.00416.x

Billman, G. E., Englert, H. C., & Schölkens, B. A. (1998). HMR 1883, a novel cardioselective inhibitor of the ATP-sensitive potassium channel. Part II: Effects on susceptibility to ventricular fibrillation induced by myocardial ischemia in conscious dogs. *The Journal of Pharmacology and Experimental Therapeutics*, *286*(3), 1465–1473.

Carmeliet, E. (1999). Cardiac ionic currents and acute ischemia: From channels to arrhythmias. *Physiological Reviews*, *79*(3), 917–1017. https://doi.org/10.1152/physrev.1999.79.3.917

Chi, L., Uprichard, A. C., & Lucchesi, B. R. (1990). Profibrillatory actions of pinacidil in a conscious canine model of sudden coronary death. *Journal of Cardiovascular Pharmacology*, *15*(3), 452–464. https://doi.org/10.1097/00005344-199003000-00016

Collins, M. N., & Billman, G. E. (1989). Autonomic response to coronary occlusion in animals susceptible to ventricular fibrillation. *The American Journal of Physiology*, *257*(6 Pt 2), H1886-1894. https://doi.org/10.1152/ajpheart.1989.257.6.H1886

Corey, S., & Clapham, D. E. (1998). Identification of native atrial G-protein-regulated inwardly rectifying K+ (GIRK4) channel homomultimers. *The Journal of Biological Chemistry*, *273*(42), 27499–27504. https://doi.org/10.1074/jbc.273.42.27499

Deutsch, N., Klitzner, T. S., Lamp, S. T., & Weiss, J. N. (1991). Activation of cardiac ATP-sensitive K+ current during hypoxia: Correlation with tissue ATP levels. *The American Journal of Physiology*, *261*(3 Pt 2), H671-676. https://doi.org/10.1152/ajpheart.1991.261.3.H671

Englert, H. C., Heitsch, H., Gerlach, U., & Knieps, S. (2003). Blockers of the ATP-sensitive potassium channel SUR2A/Kir6.2: A new approach to prevent sudden cardiac death. *Current Medicinal Chemistry. Cardiovascular and Hematological Agents*, *1*(3), 253–271. https://doi.org/10.2174/1568016033477423

366

367   Harvey, R. D., & Belevych, A. E. (2003). Muscarinic regulation of cardiac ion channels. *British Journal of*

368   *Pharmacology*, *139*(6), 1074–1084. https://doi.org/10.1038/sj.bjp.0705338

369

370   Higgins, C. B., Vatner, S. F., & Braunwald, E. (1973). Parasympathetic control of the heart. *Pharmacological*

371   *Reviews*, *25*(1), 119–155.

372

373   Inagaki, N., Gonoi, T., Clement, J. P., Namba, N., Inazawa, J., Gonzalez, G., Aguilar-Bryan, L., Seino, S., &

374   Bryan, J. (1995). Reconstitution of IKATP: An inward rectifier subunit plus the sulfonylurea receptor. *Science*

375   *(New York, N.Y.)*, *270*(5239), 1166–1170. https://doi.org/10.1126/science.270.5239.1166

376

377   Ito, H., Vereecke, J., & Carmeliet, E. (1994). Mode of regulation by G protein of the ATP-sensitive K+ channel

378   in guinea-pig ventricular cell membrane. *The Journal of Physiology*, *478 (Pt 1)*, 101–107.

379   https://doi.org/10.1113/jphysiol.1994.sp020233

380

381   Janse, M. J., & Wit, A. L. (1989). Electrophysiological mechanisms of ventricular arrhythmias resulting from

382   myocardial ischemia and infarction. *Physiological Reviews*, *69*(4), 1049–1169.

383   https://doi.org/10.1152/physrev.1989.69.4.1049

384

385   Kim, D., Watson, M., & Indyk, V. (1997). ATP-dependent regulation of a G protein-coupled K+ channel

386   (GIRK1/GIRK4) expressed in oocytes. *The American Journal of Physiology*, *272*(1 Pt 2), H195-206.

387   https://doi.org/10.1152/ajpheart.1997.272.1.H195

388

389   Koumi, S., Wasserstrom, J. A., & Ten Eick, R. E. (1995). Beta-adrenergic and cholinergic modulation of the

390   inwardly rectifying K+ current in guinea-pig ventricular myocytes. *The Journal of Physiology*, *486 (Pt 3)*, 647–

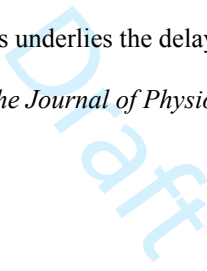391   659. https://doi.org/10.1113/jphysiol.1995.sp020841

392

393   Kurachi, Y. (1995). G protein regulation of cardiac muscarinic potassium channel. *The American Journal of*

394   *Physiology*, *269*(4 Pt 1), C821-830. https://doi.org/10.1152/ajpcell.1995.269.4.C821

395

396   Martinez, M. E., Walton, R. D., Bayer, J. D., Haïssaguerre, M., Vigmond, E. J., Hocini, M., & Bernus, O.

397   (2018). Role of the Purkinje-Muscle Junction on the Ventricular Repolarization Heterogeneity in the Healthy and

398   Ischemic Ovine Ventricular Myocardium. *Frontiers in Physiology*, *9*, 718.

399   https://doi.org/10.3389/fphys.2018.00718

400

401   Nagy, N., Szél, T., Jost, N., Tóth, A., Gy. Papp, J., & Varró, A. (2015). Novel experimental results in human

402   cardiac electrophysiology: Measurement of the Purkinje fibre action potential from the undiseased human heart.

403   *Canadian Journal of Physiology and Pharmacology*, *93*(9), 803–810. https://doi.org/10.1139/cjpp-2014-0532

404

405   Nakayama, K., Suzuki, Y., & Hashimoto, K. (1968). Sustained atrial fibrillation by acetylcholine infusion into

406   the sinus node artery. *The Tohoku Journal of Experimental Medicine*, *96*(4), 333–339.

407   https://doi.org/10.1620/tjem.96.333

408

409   Navarro-Polanco, R. A., Aréchiga-Figueroa, I. A., Salazar-Fajardo, P. D., Benavides-Haro, D. E., Rodríguez-

410   Elías, J. C., Sachse, F. B., Tristani-Firouzi, M., Sánchez-Chapula, J. A., & Moreno-Galindo, E. G. (2013).

411   Voltage sensitivity of M2 muscarinic receptors underlies the delayed rectifier-like activation of ACh-gated K(+)

412   current by choline in feline atrial myocytes. *The Journal of Physiology*, *591*(17), 4273–4286.

413   https://doi.org/10.1113/jphysiol.2013.255166

414

415   Nobles, M., Montaigne, D., Sebastian, S., Birnbaumer, L., & Tinker, A. (2018). Differential effects of inhibitory

416   G protein isoforms on G protein-gated inwardly rectifying K+ currents in adult murine atria. *American Journal*

417   *of Physiology. Cell Physiology*, *314*(5), C616–C626. https://doi.org/10.1152/ajpcell.00271.2016

418

419   Pappano, A. J., & Carmeliet, E. E. (1979). Epinephrine and the pacemaking mechanism at plateau potentials in

420   sheep cardiac Purkinje fibers. *Pflugers Archiv: European Journal of Physiology*, *382*(1), 17–26.

421   https://doi.org/10.1007/BF00585899

422

423   Recordati, G., Schwartz, P. J., Pagani, M., Malliani, A., & Brown, A. M. (1971). Activation of cardiac vagal

424   receptors during myocardial ischemia. *Experientia*, *27*(12), 1423–1424. https://doi.org/10.1007/BF02154267

425

426   Song, Y., Thedford, S., Lerman, B. B., & Belardinelli, L. (1992). Adenosine-sensitive afterdepolarizations and

427   triggered activity in guinea pig ventricular myocytes. *Circulation Research*, *70*(4), 743–753.

428   https://doi.org/10.1161/01.res.70.4.743

429

430 Terzic, A., Tung, R. T., Inanobe, A., Katada, T., & Kurachi, Y. (1994). G proteins activate ATP-sensitive K+

431 channels by antagonizing ATP-dependent gating. *Neuron*, *12*(4), 885–893. https://doi.org/10.1016/0896-

432 6273(94)90340-9

433

434 Tranum-Jensen, J., Wilde, A. A., Vermeulen, J. T., & Janse, M. J. (1991). Morphology of electrophysiologically

435 identified junctions between Purkinje fibers and ventricular muscle in rabbit and pig hearts. *Circulation*

436 *Research*, *69*(2), 429–437. https://doi.org/10.1161/01.res.69.2.429

437

438 Vajda, S., Baczkó, I., & Leprán, I. (2007). Selective cardiac plasma-membrane K(ATP) channel inhibition is

439 defibrillatory and improves survival during acute myocardial ischemia and reperfusion. *European Journal of*

440 *Pharmacology*, *577*(1–3), 115–123. https://doi.org/10.1016/j.ejphar.2007.08.016

441

442 Varró, A., & Baczkó, I. (2010). Possible mechanisms of sudden cardiac death in top athletes: A basic cardiac

443 electrophysiological point of view. *Pflugers Archiv: European Journal of Physiology*, *460*(1), 31–40.

444 https://doi.org/10.1007/s00424-010-0798-0

445

446 Varro, A., Baláti, B., Iost, N., Takács, J., Virág, L., Lathrop, D. A., Csaba, L., Tálosi, L., & Papp, J. G. (2000).

447 The role of the delayed rectifier component IKs in dog ventricular muscle and Purkinje fibre repolarization. *The*

448 *Journal of Physiology*, *523 Pt 1*, 67–81. https://doi.org/10.1111/j.1469-7793.2000.00067.x

449

450 Weiss, J. N., & Venkatesh, N. (1993). Metabolic regulation of cardiac ATP-sensitive K+ channels.

451 *Cardiovascular Drugs and Therapy*, *7 Suppl 3*, 499–505. https://doi.org/10.1007/BF00877614

452

453 Zuanetti, G., De Ferrari, G. M., Priori, S. G., & Schwartz, P. J. (1987). Protective effect of vagal stimulation on

454 reperfusion arrhythmias in cats. *Circulation Research*, *61*(3), 429–435. https://doi.org/10.1161/01.res.61.3.429

455 **Figure Legends**

456 **Figure 1.** Representative traces of Purkinje fiber (A, B) and ventricular muscle preparations

457 (C, D); 5 μM acetylcholine (red dotted lines) alone caused no changes in either preparation

458 type (A, C), while it caused significant prolongation when applied cummulatively after 5 μM

459 pinacidil (B, D, pinacidil effect represented as blue dashed lines). Bars in panel E represent

460 the values of APD_{90} in each treatment group, from top to bottom corresponding to the traces

461 A to D. Abbreviations under bars: C, control; P, pinacidil, A, acetylcholine. The pacing cycle

462 length was 500 ms. Values are mean ± SEM; *,# $p<0.05$ RM-ANOVA followed by

463 Bonferroni's post-hoc test.

464

465 **Figure 2.** Pinacidil (5 μM) increased the action potential duration dispersion (indicated by

466 ΔAPD_{90} in percentages, and in ms above the bars) between Purkinje fiber and ventricular

467 muscle preparations, while acetylcholine (5 μM), when applied after pinacidil, decreased

468 dispersion. The pacing cycle length was 500 ms.

469

470 **Figure 3.** Effect of carbachol on I_{K-ATP}. Ionic currents were measured under a slow voltage

471 ramp protocol (panel A) between -120 mV and 60 mV. The currents were analysed at 0 and

472 30 mV. Panel B demonstrates original representative current traces (left) and bar graphs

473 (right) where 3 μM carbachol (dotted line) failed to influence the control current analysed at

474 0 mV. Inset shows identical current fractions between –3 mV and 45 mV (indicated by dashed

475 rectangle). Current traces in panel C as well as in the inset, illustrate large increase of the

476 membrane current after application of 5 μM pinacidil (blue dashed line) that was inhibited by

477 the subsequently applied 3 μM carbachol (red dotted line). In bar graphs (right), asterisk

478 denotes significant change between control (left column) and pinacidil (middle column),

479 while hash tag indicates significant change between pinacidil (middle column) and carbachol

480 (right column).

481

482 **Figure 4.** Representative action potential trace (A) showing that hypoxic conditions caused

483 significant action potential duration abbreviation and decreased mean diastolic potential and

484 amplitude in canine ventricular preparations (blue dashed line), while acetylcholine (5 μM)

485 caused a significant prolongation in action potential duration (red dotted line). Values of

486 APD_{90} are represented as bars (B). Abbreviations under bars: C, control; H, hypoxia, A,

487 acetylcholine. The pacing cycle length was 500 ms. Values are mean ± SEM; *,#$p<0.05$,

488 RM-ANOVA followed by Bonferroni's post-hoc test.

489

490 **Figure 5.** Representative action potential showing the effect of acetylcholine (5 μM, red

491 dotted line) on a Purkinje fiber taken from a human donor heart (A). Values of APD_{90} are

492 represented as bars (B). Abbreviations under bars: C, control; A, acetylcholine. The pacing
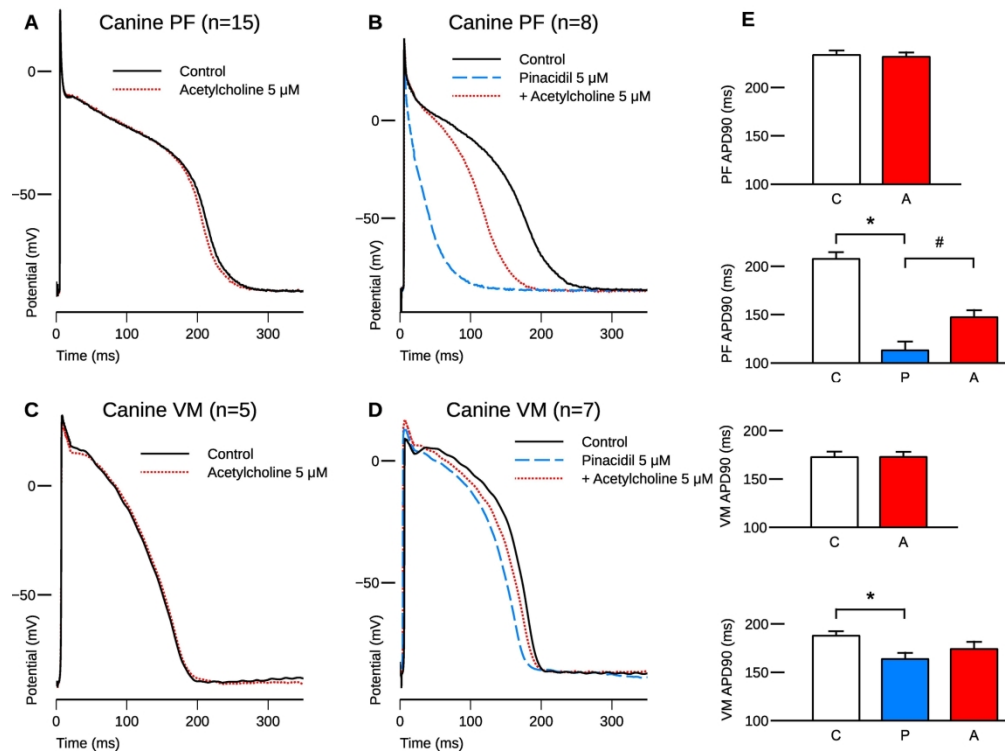
493 cycle length was 500 ms. Values are mean ± SEM.

Figure 1. Representative traces of Purkinje fiber (A, B) and ventricular muscle preparations (C, D); 5 µM acetylcholine (red dotted lines) alone caused no changes in either preparation type (A, C), while it caused significant prolongation when applied cummulatively after 5 µM pinacidil (B, D, pinacidil effect represented as blue dashed lines). Bars in panel E represent the values of APD90 in each treatment group, from top to bottom corresponding to the traces A to D. Abbreviations under bars: C, control; P, pinacidil, A, acetylcholine. The pacing cycle length was 500 ms. Values are mean ± SEM; *,# $p < 0.05$ RM-ANOVA followed by Bonferroni's post-hoc test.
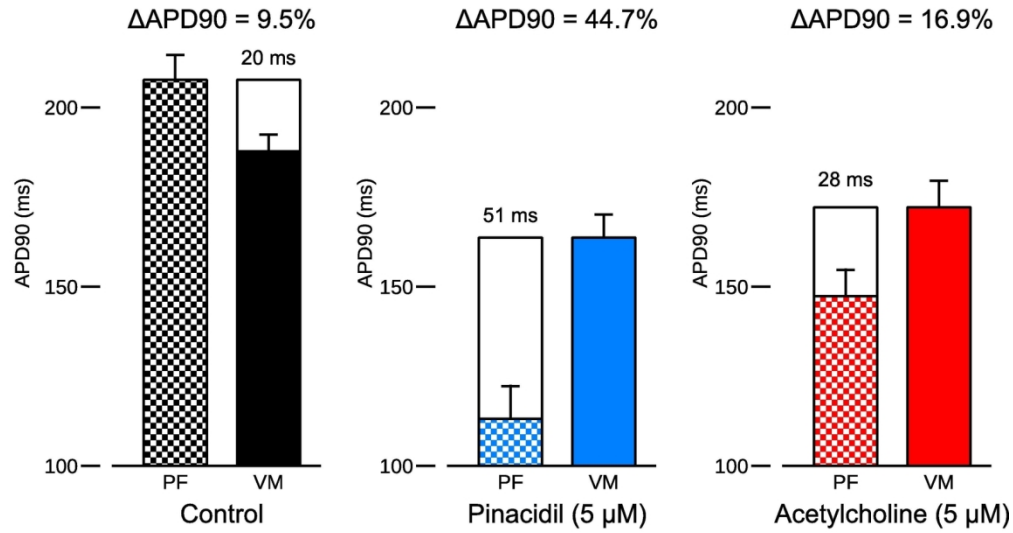
207x155mm (300 x 300 DPI)

Figure 2. Pinacidil (5 μM) increased the action potential duration dispersion (indicated by ΔAPD90 in percentages, and in ms above the bars) between Purkinje fiber and ventricular muscle preparations, while acetylcholine (5 μM), when applied after pinacidil, decreased dispersion. The pacing cycle length was 500 ms.
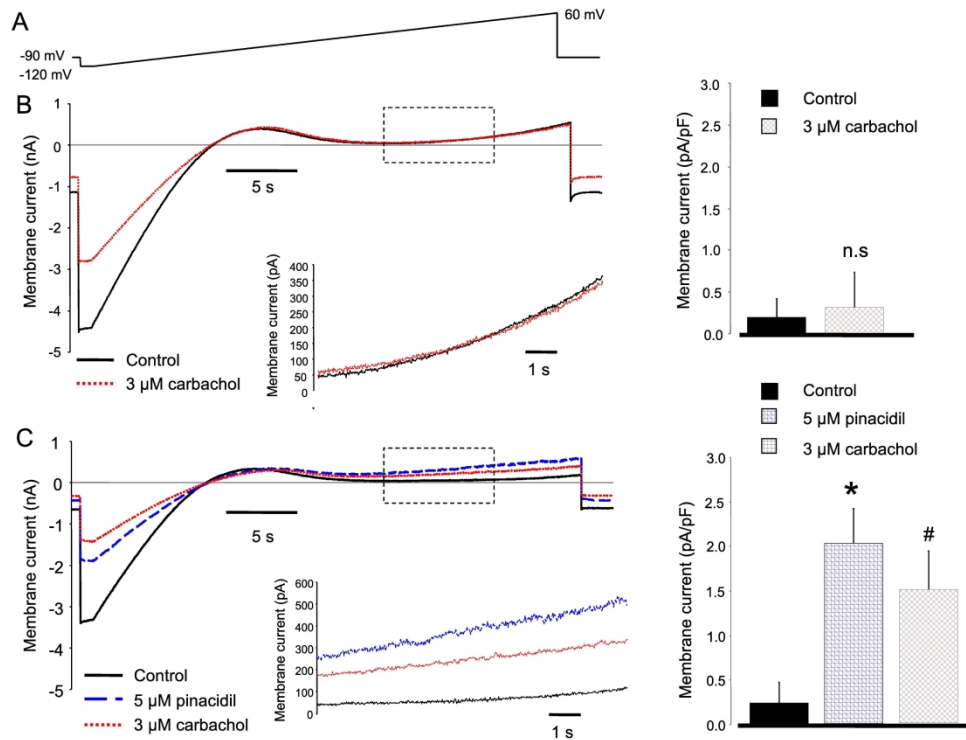
146x79mm (300 x 300 DPI)

Figure 3. Effect of carbachol on IK-ATP. Ionic currents were measured under a slow voltage ramp protocol (panel A) between -120 mV and 60 mV. The currents were analysed at 0 and 30 mV. Panel B demonstrates original representative current traces (left) and bar graphs (right) where 3 µM carbachol (dotted line) failed to influence the control current analysed at 0 mV. Inset shows identical current fractions between −3 mV and 45 mV (indicated by dashed rectangle). Current traces in panel C as well as in the inset, illustrate large increase of the membrane current after application of 5 µM pinacidil (blue dashed line) that was inhibited by the subsequently applied 3 µM carbachol (red dotted line). In bar graphs (right), asterisk denotes significant change between control (left column) and pinacidil (middle column), while hash tag indicates significant change between pinacidil (middle column) and carbachol (right column).
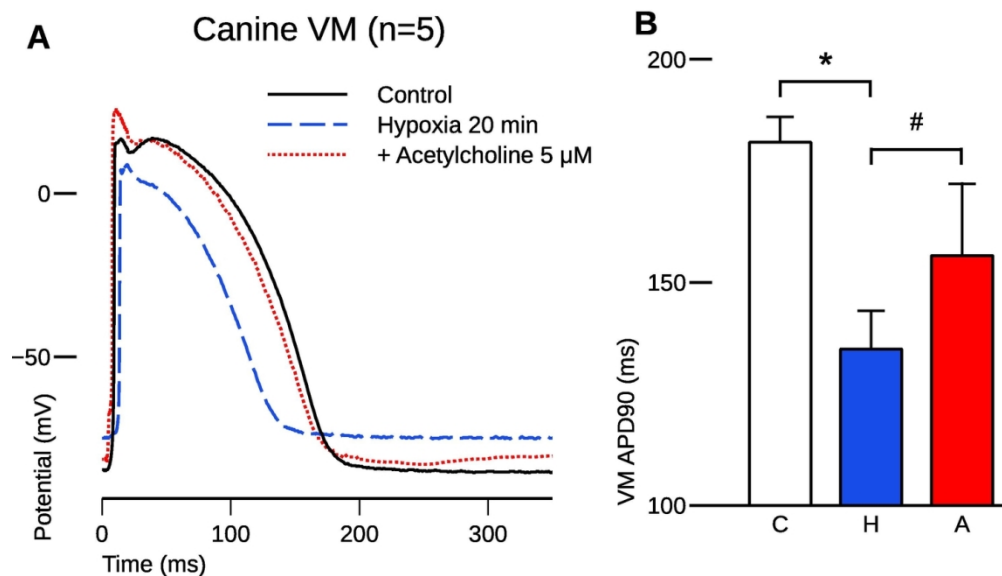
254x190mm (300 x 300 DPI)

Figure 4. Representative action potential trace (A) showing that hypoxic conditions caused significant action potential duration abbreviation and decreased mean diastolic potential and amplitude in canine ventricular preparations (blue dashed line), while acetylcholine (5 µM) caused a significant prolongation in action potential duration (red dotted line). Values of APD90 are represented as bars (B). Abbreviations under bars: C, control; H, hypoxia, A, acetylcholine. The pacing cycle length was 500 ms. Values are mean ± SEM; *,#p<0.05, RM-ANOVA followed by Bonferroni's post-hoc test.
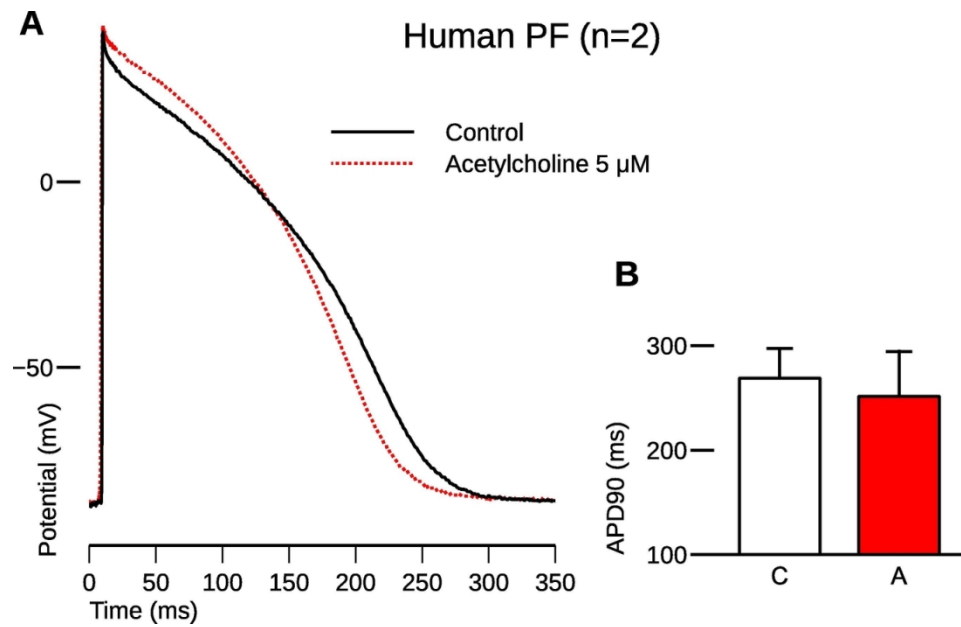
126x74mm (300 x 300 DPI)

Figure 5. Representative action potential showing the effect of acetylcholine (5 µM, red dotted line) on a Purkinje fiber taken from a human donor heart (A). Values of APD90 are represented as bars (B). Abbreviations under bars: C, control; A, acetylcholine. The pacing cycle length was 500 ms. Values are mean ± SEM.

121x74mm (300 x 300 DPI)

1

2

3

4

5

6

7

8

9

10

11
Appendix

12 **Introduction**

13 Acetylcholine has been previously shown to augment J-point elevation and to induce phase-2 reentry,

14 thus precipitating polymorphic ventricular tachycardia in preparations pretreated with agents designed

15 to pharmacologically mimic the genetic defects previously shown to be associated with the early

16 repolarization syndrome (ERS). Previously, Haïssaguerre et al. (2008) have described that extrasystolic

17 activity arising from the Purkinje network is able to precipitate ventricular tachyarrhythmias in the

18 setting of ERS. We examined Purkinje fibers under conditions pharmacologically mimicking the ion

19 channel changes caused by the genetic defects previously reported to be associated with ERS, including

20 gain of function in $I_{\text{K-ATP}}$ (*KCNJ8* and *ABCC9*) or I_{to} (*SCN1Bb and KCND3*) (Hu et al., 2014b; Barajas-

21 Martínez et al., 2014; Haïssaguerre et al., 2009) or loss of function in I_{Ca} (*CACNA1C, CACNB2* and

22 *CACNA2D1*) (Burashnikov et al., 2010; Napolitano and Antzelevitch, 2011) or I_{Na} (*SCN5A* and

23 *SCN10A*) (Watanabe et al., 2011; Hu et al., 2014a), and applied an antiarrhytmic drug successfully used

24 to treat ventricular tachyarrhythmias in ERS: cilostazol (Iguchi et al., 2013; Shinohara et al., 2014;).

25

26 **Methods**

27 *Conventional microelectrode technique*

28 All experiments were performed on canine Purkinje fibers using the conventional microelectrode

29 technique. The preparations were placed in Locke's solution and allowed to equilibrate for at least 2

30 hours while superfused (flow rate 4-5 ml/min) also with Locke's solution containing (in mM): NaCl

31 120, KCl 4, CaCl2 2, MgCl2 1, NaHCO3 22, and glucose 11. The pH of this solution was 7.40 to 7.45

32 when gassed with 95% O2 and 5% CO2 at 37 °C. All experiments were performed at 37 °C. Electrical

33 pulses of 0.5–2 ms in duration at twice the diastolic threshold in intensity (S1) were delivered to the

34 preparations through bipolar platinum electrodes at a basic cycle length of 500 ms. Transmembrane

35 potentials were recorded using glass capillary microelectrodes filled with 3 M KCl (tip resistance: 5 to

36 15 MΩ). The microelectrodes were coupled through an Ag-AgCl junction to the input of a

37 high-impedance, capacitance-neutralizing amplifier (Experimetria 2011). Intracellular recordings were

38 displayed on a storage oscilloscope (Hitachi V-555) and led to a computer system.

39

40 *Pharmacological models*

41 Our pharmacological models of the early repolarization syndrome in Purkinje fibers were based on

42 previous experiments (Koncz et al., 2014; Gurabi et al., 2014). We pharmacologically mimicked the

43 ion channel changes caused by the genetic defects associated with ERS: pinacidil (5 µM; $I_{K\text{-}ATP}$ gain of

44 function), NS5806 (7 µM; I_{to} gain of function), nisoldipine (1 µM; I_{Ca} loss of function), mexiletine

45 (20 µM; I_{Na} loss of function). The more efficacious enantiomer of mexiletine, R-mexiletine was used

46 (Gurabi et al., 2017); the concentration corresponds to a peak therapeutic plasma concentration (Varró

47 and Lathrop, 1990). The application of each compound was followed by an equilibration period,

48 enabling the tissue to reach steady-state, then the next compound was administered in a cumulative

49 manner. Acetylcholine (5 µM) was used to simulate increased parasympathetic tone. Cilostazol

50 (10 µM) was applied after acetylcholine.

51

52 **Results**

53 *Model 1: Pinacidil + acetylcholine + cilostazol (n=6)*

54 The effects of pinacidil and acetylcholine were described in the main article. Cilostazol caused a

55 notable plateau elevation without changing repolarization (Figure A1-A).

56

57 *Model 2: NS5806 + pinacidil + acetylcholine + cilostazol (n=5)*

58 Cilostazol significantly increased action potential duration (APD) when applied after NS5806, pinacidil

59 and acetylcholine (Figure A1-B).

60

61

62 *Model 3: Mexiletine + NS5806 + cilostazol (n=4)*

63 After inhibition of I_{Na} by mexiletine, followed by the activation I_{to} by NS5806 and the administration of

64 acetylcholine, cilostazol caused a slight prolongation of the APD (Figure A1-C).

65

66 *Model 4: Nisoldipine + NS5806 + acetylcholine + cilostazol (n=4)*

67 Cilostazol was also applied after nisoldipine, NS5806 and acetylcholine, causing a slight plateau

68 elevation and slight APD prolongation (Figure A1-D).

69

70 **Conclusion**

71 Since most conventional antiarrhythmic drugs, including beta-blockers, verapamil, lidocaine or

72 amiodarone, are not capable of suppressing tachyarrhythmic episodes in the early repolarization

73 syndrome, cilostazol should remain a prominent candidate in clinical trials related to early

74 repolarization. Formerly, we found I_{to} blocking ability of cilostazol (Patocskai et al., 2016) next to its

75 ability to augment I_{Ca} (Matsui et al., 1999). The above detailed normalization of the repolarization

76 defect might carry a possible therapeutic value of cilostazol in early repolarization (ER), when the

77 origin of arrhythmic activity is localized to the Purkinje system.

78   **References**

79   Barajas-Martínez, H., Hu, D., Ferrer, T., Onetti, C. G., Wu, Y., Burashnikov, E., Boyle, M., Surman, T., Urrutia, J.,

80   Veltmann, C., Schimpf, R., Borggrefe, M., Wolpert, C., Ibrahim, B. B., Sánchez-Chapula, J. A., Winters, S., Haïssaguerre,

81   M., & Antzelevitch, C. (2012). Molecular genetic and functional association of Brugada and early repolarization syndromes

82   with S422L missense mutation in KCNJ8. *Heart Rhythm*, *9*(4), 548–555. https://doi.org/10.1016/j.hrthm.2011.10.035

83

84   Burashnikov, E., Pfeiffer, R., Barajas-Martinez, H., Delpón, E., Hu, D., Desai, M., Borggrefe, M., Häissaguerre, M., Kanter,

85   R., Pollevick, G. D., Guerchicoff, A., Laiño, R., Marieb, M., Nademanee, K., Nam, G.-B., Robles, R., Schimpf, R.,

86   Stapleton, D. D., Viskin, S., … Antzelevitch, C. (2010). Mutations in the cardiac L-type calcium channel associated with

87   inherited J-wave syndromes and sudden cardiac death. *Heart Rhythm*, *7*(12), 1872–1882.

88   https://doi.org/10.1016/j.hrthm.2010.08.026

89

90   Gurabi, Z., Patocskai, B., Györe, B., Virág, L., Mátyus, P., Papp, J. G., Varró, A., & Koncz, I. (2017). Different

91   electrophysiological effects of the levo- and dextro-rotatory isomers of mexiletine in isolated rabbit cardiac muscle.

92   *Canadian Journal of Physiology and Pharmacology*, *95*(7), 830–836. https://doi.org/10.1139/cjpp-2016-0599

93

94   Haïssaguerre, M., Chatel, S., Sacher, F., Weerasooriya, R., Probst, V., Loussouarn, G., Horlitz, M., Liersch, R., Schulze-

95   Bahr, E., Wilde, A., Kääb, S., Koster, J., Rudy, Y., Le Marec, H., & Schott, J. J. (2009). Ventricular fibrillation with

96   prominent early repolarization associated with a rare variant of KCNJ8/KATP channel. *Journal of Cardiovascular*

97   *Electrophysiology*, *20*(1), 93–98. https://doi.org/10.1111/j.1540-8167.2008.01326.x

98

99   Haïssaguerre, M., Derval, N., Sacher, F., Jesel, L., Deisenhofer, I., de Roy, L., Pasquié, J.-L., Nogami, A., Babuty, D., Yli-

100   Mayry, S., De Chillou, C., Scanu, P., Mabo, P., Matsuo, S., Probst, V., Le Scouarnec, S., Defaye, P., Schlaepfer, J.,

101   Rostock, T., … Clémenty, J. (2008). Sudden cardiac arrest associated with early repolarization. *The New England Journal*

102   *of Medicine*, *358*(19), 2016–2023. https://doi.org/10.1056/NEJMoa071968

103

104   Hu, D., Barajas-Martínez, H., Pfeiffer, R., Dezi, F., Pfeiffer, J., Buch, T., Betzenhauser, M. J., Belardinelli, L., Kahlig, K.

105   M., Rajamani, S., DeAntonio, H. J., Myerburg, R. J., Ito, H., Deshmukh, P., Marieb, M., Nam, G.-B., Bhatia, A., Hasdemir,

106   C., Haïssaguerre, M., … Antzelevitch, C. (2014). Mutations in SCN10A are responsible for a large fraction of cases of

107   Brugada syndrome. *Journal of the American College of Cardiology*, *64*(1), 66–79.

108   https://doi.org/10.1016/j.jacc.2014.04.032

109

110   Hu, D., Barajas-Martínez, H., Terzic, A., Park, S., Pfeiffer, R., Burashnikov, E., Wu, Y., Borggrefe, M., Veltmann, C.,

111   Schimpf, R., Cai, J. J., Nam, G.-B., Deshmukh, P., Scheinman, M., Preminger, M., Steinberg, J., López-Izquierdo, A.,

112   Ponce-Balbuena, D., Wolpert, C., … Antzelevitch, C. (2014). ABCC9 is a novel Brugada and early repolarization syndrome

113   susceptibility gene. *International Journal of Cardiology*, *171*(3), 431–442. https://doi.org/10.1016/j.ijcard.2013.12.084

114

115   Iguchi, K., Noda, T., Kamakura, S., & Shimizu, W. (2013). Beneficial effects of cilostazol in a patient with recurrent

116   ventricular fibrillation associated with early repolarization syndrome. *Heart Rhythm*, *10*(4), 604–606.

117   https://doi.org/10.1016/j.hrthm.2012.11.001

118

119   Koncz, I., Gurabi, Z., Patocskai, B., Panama, B. K., Szél, T., Hu, D., Barajas-Martínez, H., & Antzelevitch, C. (2014).

120   Mechanisms underlying the development of the electrocardiographic and arrhythmic manifestations of early repolarization

121   syndrome. *Journal of Molecular and Cellular Cardiology*, *68*, 20–28. https://doi.org/10.1016/j.yjmcc.2013.12.012

122

123   Matsui, K., Kiyosue, T., Wang, J. C., Dohi, K., & Arita, M. (1999). Effects of pimobendan on the L-type Ca^{2+} current and

124   developed tension in guinea-pig ventricular myocytes and papillary muscle: Comparison with IBMX, milrinone, and

125   cilostazol. *Cardiovascular Drugs and Therapy*, *13*(2), 105–113. https://doi.org/10.1023/a:1007779908346

126

127   Napolitano, C., & Antzelevitch, C. (2011). Phenotypical manifestations of mutations in the genes encoding subunits of the

128   cardiac voltage-dependent L-type calcium channel. *Circulation Research*, *108*(5), 607–618.

129   https://doi.org/10.1161/CIRCRESAHA.110.224279

130

131   Patocskai, B., Barajas-Martinez, H., Hu, D., Gurabi, Z., Koncz, I., & Antzelevitch, C. (2016). Cellular and ionic

132   mechanisms underlying the effects of cilostazol, milrinone, and isoproterenol to suppress arrhythmogenesis in an

133   experimental model of early repolarization syndrome. *Heart Rhythm*, *13*(6), 1326–1334.

134   https://doi.org/10.1016/j.hrthm.2016.01.024

135

136   Shinohara, T., Ebata, Y., Ayabe, R., Fukui, A., Okada, N., Yufu, K., Nakagawa, M., & Takahashi, N. (2014). Combination

137   therapy of cilostazol and bepridil suppresses recurrent ventricular fibrillation related to J-wave syndromes. *Heart Rhythm*,

138   *11*(8), 1441–1445. https://doi.org/10.1016/j.hrthm.2014.05.001

139

140   Varró, A., & Lathrop, D. A. (1990). Sotalol and mexiletine: Combination of rate-dependent electrophysiological effects.

141   *Journal of Cardiovascular Pharmacology*, *16*(4), 557–567. https://doi.org/10.1097/00005344-199010000-00006

142

143   Watanabe, H., Nogami, A., Ohkubo, K., Kawata, H., Hayashi, Y., Ishikawa, T., Makiyama, T., Nagao, S., Yagihara, N.,

144   Takehara, N., Kawamura, Y., Sato, A., Okamura, K., Hosaka, Y., Sato, M., Fukae, S., Chinushi, M., Oda, H., Okabe, M., …

145   Makita, N. (2011). Electrocardiographic characteristics and SCN5A mutations in idiopathic ventricular fibrillation

146   associated with early repolarization. *Circulation. Arrhythmia and Electrophysiology*, *4*(6), 874–881.

147   https://doi.org/10.1161/CIRCEP.111.963983

148

149 **Appendix figure legend**

150 **Figure A1.** Representative action potential traces from canine Purkinje fibers showing the effects of

151 10 μM cilostazol (continuous lines) in the following models of the early repolarization syndrome (ERS,

152 dotted lines): pinacidil 5 μM + acetylcholine 5 μM (Model 1; A), NS5806 7 μM + pinacidil 5 μM +

153 acetylcholine 5 μM (Model 2; B), mexiletine 20 μM + NS5806 7 μM (Model 3; C), and nisoldipine
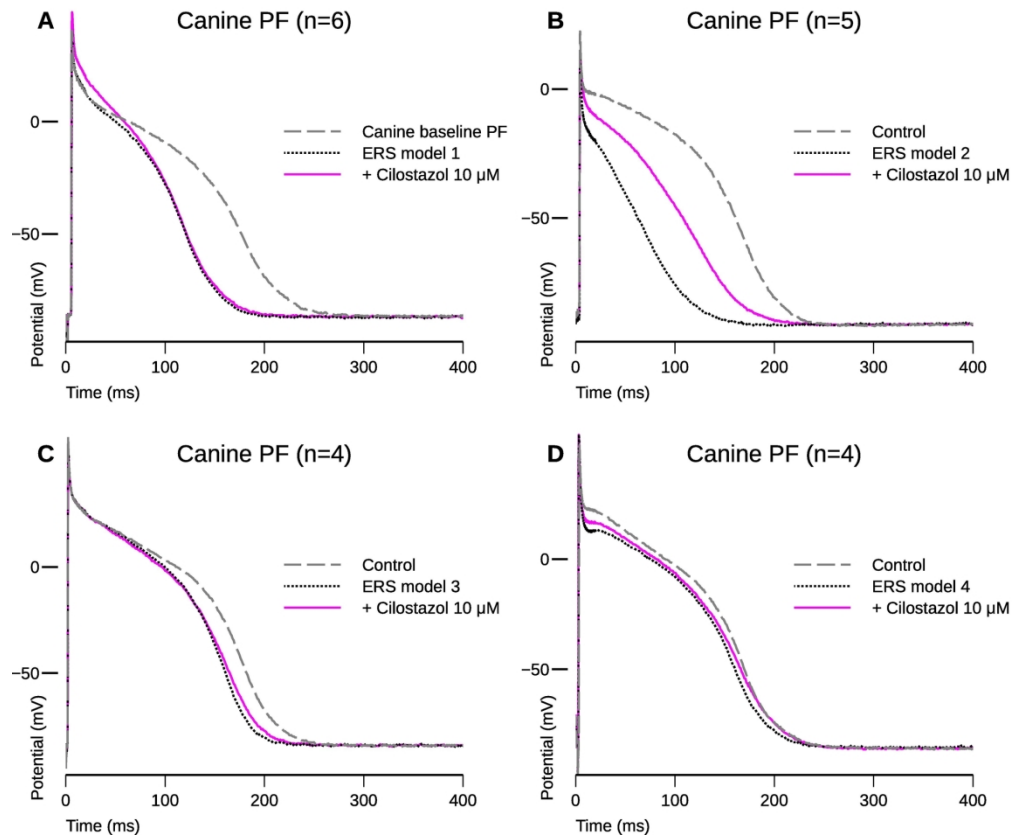
154 1 μM + NS5806 7 μM + acetylcholine 5 μM (Model 4; D).

Figure A1. Representative action potential traces from canine Purkinje fibers showing the effects of 10 μM cilostazol (continuous lines) in the following models of the early repolarization syndrome (ERS, dotted lines): pinacidil 5 μM + acetylcholine 5 μM (Model 1; A), NS5806 7 μM + pinacidil 5 μM + acetylcholine 5 μM (Model 2; B), mexiletine 20 μM + NS5806 7 μM (Model 3; C), and nisoldipine 1 μM + NS5806 7 μM + acetylcholine 5 μM (Model 4; D).

177x149mm (300 x 300 DPI)